Sequencing individual genomes with recurrent genomic disorder deletions reveals genes for autosomal recessive traits

Bo Yuan [1,2,10], Katharina Schulze[1], Nurit Assia Batzir [1], Jefferson Sinson [1], Hongzheng Dai[1,2], Wenmiao Zhu [1,2], Francia Bocanegra [3], Chin-To Fong [4], Jimmy Holder [5], Joanne Nguyen [6], Christian P. Schaaf [1,7], Yaping Yang [1,2], Weimin Bi [1,2], Christine Eng [1,2], Chad Shaw [1,2], James R. Lupski [1,5,8,9], Pengfei Liu [1,2]

[1] Department of Molecular and Human Genetics, Baylor College of Medicine, Houston, TX, USA
[2] Baylor Genetics, Houston, TX, USA
[3] Instituto de Referencia Andino, Bogotá, Colombia
[4] Department of Pediatrics, University of Rochester Medical Center, Rochester, NY, USA
[5] Department of Pediatrics, Baylor College of Medicine, Houston, TX, USA
[6] Department of Pediatrics, University of Texas Health Science Center, Houston, TX, USA
[7] Institute of Human Genetics, Heidelberg University, Heidelberg, Germany
[8] Human Genome Sequencing Center, Baylor College of Medicine, Houston, TX
[9] Texas Children's Hospital, Houston, TX
[10] Present Address: Seattle Children's Hospital, Seattle, WA.

[*]To whom correspondence should be addressed:
Pengfei Liu, PhD
Molecular and Human Genetics
Baylor College of Medicine
One Baylor Plaza
Houston, TX 77030
Phone: (713) 798-5122
Email: pengfeil@bcm.edu

Abstract

In medical genetics, discovery and characterization of disease trait contributory genes and alleles depends on genetic reasoning, study design, and patient ascertainment. We present novel genomic insights to enhance discovery in the challenging context of autosomal recessive (AR) traits and bi-allelic variation. We demonstrate computationally that new mutation mediated by nonallelic homologous recombination (NAHR), involving recurrent deletions at 30 genomic regions, likely drives recessive disease burden for over 70% of loci within these segmental deletions or at least 2% of loci genome wide. Meta-analyses of literature-reported patients implicate that NAHR-deletions are depleted from the ascertained pool of AR trait alleles. Exome reanalysis on subjects harboring recurrent deletions uncovered new disease-contributing variants in genes including *COX10*, *ERCC6*, *PRRT2* and *OTUD7A*. Our data demonstrate that genomic sequencing of personal genomes with NAHR-deletions could dramatically foment allele and gene discovery, enhance clinical molecular diagnosis, and could potentially enable human haploid genetics screens.

Introduction

Over the last few decades, efforts to decipher molecular and genetic mechanisms underlying Mendelian conditions have repeatedly demonstrated that mutations aggregate in personal genomes and lead to human diseases in a continuum of allelic modalities, ranging from monoallelic (dominant), biallelic (recessive), triallelic, to multiallelic and more complex modes of inheritance (Lupski et al. 2011; Lupski 2021). Recent large-scale family-based genomic studies using exome sequencing (ES) have uncovered hundreds of new disease loci, with the majority following traditional Mendelian inheritance, i.e., monoallelic (AD) or biallelic (AR) trait segregation (Posey et al. 2019). Although optimism has been increasing towards achieving disease annotation for a substantial portion of the haploinsufficient part of the human genome through dominant disease gene discoveries, statistical analysis from rare disease cohort studies suggests that the trajectory to understand the recessive or biallelic-disease-causing portion of the human genome is less certain (Martin et al. 2018; Bamshad et al. 2019; Cacheiro et al. 2020).

This apparent discrepancy in discovery between dominant and recessive trait genes can perhaps most parsimoniously be explained by the Clan Genomics Model (Lupski et al. 2011). The model predicts that dominant diseases are largely caused by emergence of new alleles in recent generations, *i.e. de novo* mutations (DNMs). Differently, recessive diseases arise when a *pair* of disease alleles at a locus are aggregated in a personal genome in the *trans* configuration by transmission genetics; the incidence of disease correlates with the product of the probabilities of sampling each of the two alleles, whether existing in a population or *de novo*, in a mating. Because of the bivalent nature, the overall incidence of a recessive trait depends on the local allelic architecture, i.e., the snapshot of the frequency distribution of all pathogenic alleles. This

is a characteristic not observed in dominant traits, where individual alleles act in solitude and the overall incidence mostly depends on new mutations.

Individual recessive alleles can emerge and be carried in populations, clans and pedigrees with no impact on phenotype. Consequently, some recessive disease alleles can reach high population allele frequencies [e.g., $8x10^{-4}$ for NM_000520.6(*HEXA*):c.1274_1277dup (p.Tyr427fs), the most common Tay Sachs disease allele], which can be several orders of magnitude higher than alleles associated with dominant disease traits (~10^{-8} as an estimate for the *de novo* single nucleotide variant rate). As one may expect, previous research efforts or clinical testing in unselected cohorts are likely to ascertain recessive diseases with at least one allele of high population frequency. In contrast, if a yet-to-be-defined recessive disease trait gene does not have appreciable pathogenic alleles represented at a sufficient population frequency, disease discovery and annotation of the gene would be greatly hampered due to the extremely low incidence and difficulty in ascertaining affected individuals, even when considering a world-wide population of 7.8 billion.

Special strategies and genomic approaches need to be implemented to overcome this potential roadblock in discovery and characterization initiatives. Ascertaining patients in populations with an elevated coefficient of consanguinity and autozygosity is a widely applied and highly successful strategy for recessive disease gene discovery. In this circumstance, the allele pool shrinks to the Clan of the patient's extended family, which dramatically escalates the effective disease-allele frequency (Gonzaga-Jauregui et al. 2020; Alkuraya 2021). Thus, the probability of ascertaining patients with the recessive trait disorder increases exponentially, even when all

existing alleles are ultra-rare in sampling the general population (Coban-Akdemir et al. 2020). Similarly, focusing on a specific geographic or ethnic population is another effective strategy, often attributed to available founder mutation alleles in the population studied (Gonzaga-Jauregui et al. 2020).

Here, we present an alternative study design strategy to enhance the investigation of new disease genes and alleles in recessive traits that are difficult to access by conventional methods. This strategy leverages sequencing of loss-of-function (LoF) alleles caused by large recurrent genomic deletions rendering a locus haploinsufficient. Recurrent genomic deletions are a subset of contiguous gene deletions that are characterized by a special type of mutational mechanism called nonallelic homologous recombination, or NAHR (Lupski 2019). NAHR is mediated by ectopic recombination between highly similar repeat sequences termed low-copy repeats (LCRs) or segmental duplications (SDs) (Liu et al. 2012). The human genome is evolutionarily structured to be highly enriched for SDs, which creates a large number of architectural hotspots for genomic disorders and mirror traits to emerge (Lupski 2015b; Dennis and Eichler 2016).

Recurrent genomic deletions (or NAHR-deletions) set up an ideal background for recessive disease gene discovery due to a key property: they act as highly prevalent recessive alleles in comparison to other small variant, i.e. single nucleotide variants (SNV) and indels, recessive disease alleles and they continue to renew because of high mutation rates of structural variant mutagenesis. It has been shown that the mutation rate of NAHR at a given locus can be as high as ~10^{-4} to 10^{-5}, which is orders of magnitudes higher than new mutation rates from SNVs and indels (Turner et al. 2008). The high new mutation rate ensures that these genomic deletions

continuously arise *de novo* in the human population among unrelated individuals (Berg et al. 2010; Beck et al. 2019). This 'recurrent' nature of genomic deletions distinguishes them from the other recessive disease alleles that are more 'stationary' or artifacts of past population history amplified by recent population expansion. Moreover, as genotyping assays are performed on relatives of patients with deletions as well as on individuals without a disease indication, we recognize that many recurrent genomic deletions are incompletely penetrant (Potocki et al. 1999; Rosenfeld et al. 2013; Stefansson et al. 2014; Wu et al. 2015; Crawford et al. 2019; Yang et al. 2019; Collins et al. 2020; Ren et al. 2020), i.e., the fitness of the deletion allele can be high, at least in certain genomic backgrounds (Lupski 2015a; Mannik et al. 2015). Thus, we hypothesized that because of these key attributes, population prevalence and new mutation rate, NAHR alleles are contributing to a considerable fraction of recessive diseases and are perhaps among the most important alleles at these recessive trait loci. Additionally, we hypothesize that although the sequencing of large recurrent deletions has resulted in isolated characterizations of new recessive genes and alleles in the past, such efforts have been under-recognized as a concerted generalizable study strategy, possibly due to the preconceived notion that most of the large recurrent deletions are 'dominant' incompletely penetrant disease alleles.

To pursue these hypotheses, we formulated a large computational analysis using both genome-wide population data resources as well as clinical genomics information (Figure 1). We demonstrate, using computational and sequencing analyses, that recurrent NAHR-deletions contribute to a major fraction of individual disease burden for over 2% of known recessive trait genes or 70% of known recessive diseases in regions encompassed by LCRs (Figure 2). By meta-analysis of all patients and disease alleles reported in the literature from the top recessive

genes predicted to be driven by NAHR-deletion alleles, we present evidence that the sequencing of individuals with recurrent deletions is under-utilized. The findings regarding allelic architecture of diseases, leveraging new mutation and the high incidence of recurrent genomic deletion alleles, can prime powerful future strategies for recessive disease gene and allele discoveries exploiting the concept of 'human haploid genetics' by investigating genomic intervals of recurrent segmental aneusomy.

Results

NAHR-deletion: the most prevalent allele for interval mapped recessive trait genes

In order to systematically evaluate the contribution of recurrent genomic deletions to autosomal recessive conditions, we first mapped all possible loci that are susceptible to recurrent deletions caused by NAHR between directly oriented SDs (Dittwald et al. 2013) using the GRCh38 human reference genome sequence (Figure S1, Table S1). The collapsed NAHR map contains 717 unique recurrent deletion regions. We enumerated the subset of recurrent deletion events with available data from screening efforts in the literature or clinical testing to substantiate a prevalence estimate, and focused the subsequent analyses on these regions (n=51). We identified 30 deletions with a maximal population prevalence over 1/1,000,000 based on estimates from the UK Biobank, the Icelandic, and the gnomAD SV studies (Stefansson et al. 2014; Crawford et al. 2019; Collins et al. 2020) (Table 1, Table S2). These 30 deletions span 64 Mb of unique genomic sequences, contribute to an aggregate population allele burden of 1.3%, and encompass 1517 genes, of which 78 are known to cause recessive disorders. An additional 21 deletions, with populational prevalence possibly lower than 1/1,000,000, are also identified to recur in high prevalence if a clinical cohort is ascertained (Table S2). With the 21 ultra-rare deletions

included, the span of genomic coverage increases to 82 Mb; the number of genes involved becomes 1828, with 100 representing established recessive disease trait genes.

We then catalogued, based on existing knowledge and datasets, a compendium of all reported and predicted carrier alleles for each known recessive trait gene in the human genome. Our objective for this recessive allele catalog is to estimate and dissect the impact of recurrent genomic deletions' contribution to the overall disease burden. Based on mode of inheritance curations from OMIM, DECIPHER, and ClinGen, a totality of 2657 recessive disease trait genes were assembled. The carrier allele burden for each 'recessive trait gene' was calculated by summing up frequencies of unique alleles for all high-quality pathogenic variants from ClinVar, all structural variants (SV) predicted to be LoF from gnomAD SV v2.1, all high-confidence LoF small variants identified in gnomAD v3.1, and the NAHR-mediated recurrent genomic deletions, if applicable. An aggregate of 85,063 small variant and large deletion carrier alleles were identified for the 2657 genes (Table S3). For the 78 known recessive genes in the NAHR deletion regions, the number of per gene pathogenic alleles range from 1 to 308, with a median of 14. As a comparison, the remaining 2510 known recessive genes have a similar median per gene pathogenic allele count, 13, but a wider range, from 1 to 3562.

A limitation of this calculation is that SNV pathogenic missense, in-frame indel, or intronic variants not currently reported in ClinVar are inadvertently omitted. However, we argue that carrier alleles not represented in ClinVar tend to have lower allele frequencies and thus do not have a major impact on the subsequent carrier burden estimates. We further argue that the alleles that receive an entry and curation in ClinVar have higher frequencies – and therefore greater

impact on recessive disease, and these are the alleles more easily ascertained in screening tests of clinical diagnostic laboratories. This latter contention is supported by the aggregate gene-level carrier allele burden from our analysis matching empirical experience in genetic testing carrier screenings results (Table S4).(Haque et al. 2016)

Nevertheless, to account for potential unrepresented alleles from recessive genes that have not been scrutinized by large-scale systematic clinical or research screening, in the subsequent analyses, we supplemented the disease allele pool for each gene with a 10% extra variant load, comprised of ten hypothetical variants each accounting for 1% of the overall carrier burden (see Methods) for each gene. Of note, the NAHR deletion alleles rank as the most (47/78) or second most (12/78) frequent (highest population allele frequency) carrier alleles together comprising over three quarters of known recessive genes within NAHR regions! Even with the above-mentioned conservative padding to represent ten hypothetical alleles not yet ascertained, the NAHR alleles still contribute to greater than 10% of the total gene-level carrier allele burden for 58 of the 78 genes (Table S5).

NAHR-deletions contribute a major fraction of recessive disease load

It is important to note that, for a recessive trait, the population frequency and relativized frequency of a particular allele from a pool of alleles (**Fa**, fraction of allele burden) is not linearly correlated with the probability of sampling a patient with the specific allele from a group of patients (**Fd**, fraction of the disease burden). The distribution of alleles in affected individuals is determined by the pairwise allele frequency products in a pool. Thus, we calculated allelic contributions to recessive disease load using an n x n Punnett square, where n is the number of

carrier alleles for a recessive trait gene. The calculated NAHR-deletion contribution to disease can be calculated from the matrix. We denote as Fd the modeled probability of sampling one affected individuals carrying at least one recurrent deletion allele from a pool of patients affected with the recessive condition caused by the same gene. We empirically considered a gene to be under significant NAHR-deletion burden for population prevalence of the associated recessive disease, if the recurrent genomic deletion is expected in greater than 20% of all patients with this recessive disorder. By this definition, 71% (56/78) of NAHR-region recessive genes, which account for 2.11% of all known recessive genes, are under significant NAHR-deletion burden for recessive disease prevalence (Table 2)! In the context of the other alleles from the same gene, the disease contribution of the NAHR-deletion (Fd) ranks at the top for 47 genes, and at the second place for 12 more genes. The Fd scores of the top-3 alleles are listed in Table 2 and Table S5 to illustrate a snapshot of the allelic architecture for each recessive trait gene.

We next defined a log-scaled index we termed the NAHR-deletion's Impact to Recessive Disease (NIRD), to depict the gene-level disease load contribution of the NAHR allele relative to an allele with a median level of contribution to the same gene among all population carrier alleles (See Methods section). A positive NIRD score predicts that the NAHR-deletion allele plays a predominant (above the typical allele) role among all carrier alleles of the gene in disease contribution, whereas a negative score predicts a minor (below typical) role. Known recessive genes in the recurrent deletion region tend to have high NIRD scores, with 85% (66/78) scoring above 0, and 74% (58/78) scoring above 2. The two highest NIRD scores are found in *RBM8A* and *NPHP1*, 9.8 and 7.7, respectively. Both are extremely large values considering the NIRD is log-scaled.

To appreciate the properties of the NIRD scores, we adjusted the algorithm to calculate the disease contribution of any given pathogenic allele for a recessive gene, as an Allelic Impact to Recessive Disease (AIRD) score. The most common carrier allele observed in cystic fibrosis, NM_000492.3(*CFTR*):c.1521_1523delCTT (p.Phe508delPhe), also known as the ΔF508 allele, has an AIRD score of 7.3; the third most common carrier allele for Niemann-Pick disease type A, NM_000543.5(*SMPD1*):c.996del (p.Phe333fs), has an AIRD score of 2; a well-known founder mutation observed in ~10% of patients of Ashkenazi Jewish descent with Tay-Sachs disease, NM_000520.6(*HEXA*):c.1421+1G>C, has an AIRD score of -0.15, due to its lower allele frequency of 1.97×10^{-5} in the general population according to gnomAD v3.1.

The NIRD and related findings provide computational framework that supports two consequences. First, for the ~2% of known human recessive genes genome-wide or 70% of recessive genes in NAHR regions, one of the most effective but under-utilized strategies for identifying novel disease-causing alleles from human subjects is to sequence affected individuals carrying the heterozygous recurrent genomic deletion encompassing the gene of interest. Second, there likely exist uncharacterized recessive disease trait genes that may be most effectively identified by sequencing individuals bearing prevalent recurrent genomic deletions -- i.e. any of the 1439 genes within these deletion regions may have yet to be assigned an AR disease trait and could be novel biallelic/recessive disease trait genes.

<u>Meta-analysis suggests under-representation of the NAHR-deletion allele in currently discovered recessive disease allele pools</u>

The striking prediction of the high contribution of NAHR-deletions to relevant recessive disease load is seemingly contradictory to our current impression of the recessive allele landscapes, which led us to hypothesize that the NAHR-deletion alleles are currently under-represented in disease characterization efforts. To test this hypothesis, we analyzed the distributions of a near-complete catalogue of currently discovered disease alleles in 170 patient families affected with one of the recessive disorders whose carrier burden are predicted to be almost exclusively from NAHR-mediated large deletions (Fd > 70% from Table 2). The cohorts are assembled by meta-analysis of all literature reports for patients with the corresponding recessive disorder recorded in HGMD (version 2020.4). *NPHP1,* the top-ranking gene from Table 2, was not included because it is a well-characterized disease gene and therefore literature reported patients may not represent the natural disease allele composition in the world.

It is expected that all patients with biallelic disease variants fall into three categories (1) HMZ: those affected with homozygous small variants possibly from a close- or distant- consanguineous relationship, (2) SNV+SNV: those affected with compound heterozygous small variants, and (3) NAHR+SNV: those affected with a large deletion in *trans* with a small variant. We anticipate that category #1-HMZ accounts for a substantial proportion, demonstrating the well-established robustness of autozygosity mapping as a method for allelic and new recessive gene discovery (as populational rare alleles can be escalated to much higher clan allele frequency) (Coban-Akdemir et al. 2020). In outbred pedigrees and populations corresponding to categories #2-SNV+SNV and #3-NAHR+SNV, our modeling from the NIRD hypothesis is that #3-NAHR+SNV should account for a higher fraction. The opposing trend would suggest that our current disease

gene/allele discovery efforts are not exploiting the large deletion allele to the fullest extent that a 'human haploid genetics' approach might allow.

All the genes except for *RBM8A* show a poor representation for the #3-NAHR+SNV configuration, based on the 93 families when excluding the individuals affected *RBM8A* from the entire cohort (Table S6). Note that since most of the variants reported in these families are only documented once in affected human subjects, we cannot rule out the possibility that some of these variants are not causative to the clinical presentation, i.e., the variants of interest are not pathogenic. Almost 70% (64/93) of these patients carry homozygous disease alleles. Based on our modeling and the assumption of random mating, patients with homozygous variants are expected to account for a small fraction of the overall cohort, ranging from 0.53% to 5.4% per gene. However, the observed fractions of homozygotes for each gene are 1.9 to 189 (median 47) fold higher than expected. Furthermore, all of the 65 homozygous variants are rare, with 42 being ultra-rare (as defined by not observed in gnomAD v3.1). The collective patterns suggest that current efforts investigating these recessive traits tend to ascertain patients from populations with elevated autozygosity or from targeted population groups with their ethnic-specific disease founder alleles.

To avoid potential confounding factors from study designs and patient ascertainment methods, we removed patients with homozygous variants and focused on those with compound heterozygous variants. Our modeling predicts that for these top-ranking genes analyzed, the number of patients with NAHR+SNV should be 2.8 to 20 (median 12) fold higher than the number of patients with compound heterozygous small variants (Table S6). The observed counts

from many individual genes are too low to support a meaningful conclusion, but in aggregate, we have identified fewer patients with NAHR+SNV (13) compared with patients with compound heterozygous small variants (16). The recurrent deletions involved are 16p13.11 (n=4), 17p12-HNPP (n=3), DiGeorge 22q11.2 (n=2), 10q11.21q11.23 (n=2), 1q21.1-TAR (n=1), and proximal 16p11.2 (n=1). The poor representation of deletion bearing patients shows a bias that under-represents category #3-NAHR+SNV and deviates from the expectation driven by our analysis using population allele frequencies and the NIRD score.

RBM8A is the only gene from our analysis that demonstrated a discovery pattern favoring #3-NAHR-SNV, with the majority (95%, 73/77) of patients affected with the *RBM8A*-thrombocytopenia absent radius (TAR; OMIM #274000) syndrome being compound heterozygous for the 1q21.1-TAR deletion and a small variant, whereas no patients were found to carry homozygous *RBM8A* pathogenic variants (Table S6). This finding is consistent with our computational modeling based on the allele spectra illustrating an overwhelming fraction of contribution of the 1q21.1 NAHR-deletion at the disease locus (Tables 2 and S6). Moreover, the proper representation of NAHR-deletion discovery at this locus in contrast to other loci is expected because of a unique characteristic of the *RBM8A*-1q21 locus. The disease presentation requires a combination of the rare 1q21 NAHR-deletion null allele and a common (~1% minor allele frequency) hypomorphic small variant (Albers et al. 2012). However, neither of the two allele types can be found in patients as homozygotes – the NAHR-deletion homozygotes are lethal and the homozygous hypomorphic small variants are not disease-triggering. The unique molecular allele architecture and disease pathogenic mechanism of *RBM8A*, a condition that is clinically uniform and genetically homogeneous, shuts the door of discovery by sequencing of

population with high autozygosity, but spontaneously presented the #3-NAHR+SNV configurations for research discovery (Klopocki et al. 2007).

A human haploid genetics and genomics approach to recessive trait genes

We retrospectively analyzed two existing clinical cohorts to find data that test our computational prediction of NAHR-deletions conferring a major disease burden to many recessive traits. The configuration of the two cohorts are not optimized for discovery, but seem to have provided preliminary evidence in support of our prediction from computational modeling. The first cohort was assembled focusing on the *COX10* gene, defects of which cause mitochondrial complex IV deficiency (OMIM# 220110) inherited in an autosomal recessive manner. *COX10* is located within the 17p12 recurrent deletion, associated with hereditary neuropathy with liability to pressure palsies (HNPP, OMIM# 162500), a mild form of peripheral neuropathy or a dominant susceptibility locus to neuropathy after traumatic injury akin to an animal model observed as the Wallerian degeneration slow phenotype modeled in the *Wld* triplication mouse (Coleman et al. 1998). HNPP is due to decreased dosage of the *PMP22* gene via haploinsufficiency and is inherited liability to pressure palsies originally described in the Dutch population; it is often only manifested clinically as multifocal neuropathy elicited after sustained trauma to a peripheral nerve that traverses close to the body surface and manifest an entrapment neuropathy(Tyson et al. 1996) or an operative carpal tunnel syndrome co -segregating through multiple generations (Potocki et al. 1999). *PMP22* maps within the HNPP deletion and *COX10* is the only gene in the deletion interval with a known disease association other than *PMP22*. Based on our calculation, ~77% of all patients affected with biallelic *COX10* pathogenic alleles in an outbred population carry one HNPP deletion (Table 2).

We retrospectively investigated results from 596 patients suspected with a mitochondrial disorder who were clinically tested for *COX10* coding region sequencing and deletion/duplication analysis. The strength of patient assertation strategy from this cohort is that patients were referred based on clinical suspicion and therefore the distribution of pathogenic alleles from this cohort is likely free of molecular bias. A weakness of this cohort configuration is that the selected disease phenotype is of high genetic heterogeneity, which inherently predicts that only a small number of patients will indeed be affected with *COX10*-related conditions. Nevertheless, we found two patients received a possible diagnostic finding in *COX10*, both carrying the HNPP deletion as one allele. In subject #1, a hemizygous variant resulting in an in-frame small duplication of two amino acids, c.1277_1282dup (p.M426_L427dup) in exon 7 of *COX10*, was identified in *trans* to the HNPP deletion (Figure S2). Subject #2, whose referral indication is COX deficiency, has a rare VUS c.858G>T (p.W286C) in *COX10* in *trans* with the HNPP deletion. In the remaining patients without a definitive molecular diagnosis, two patients were found to have the heterozygous HNPP deletions, but a second hit in *COX10* was not found, although we cannot rule out the possibility of additional findings in intronic or regulatory regions. These findings, though under-powered, are consistent with our prediction that most patients with COX10 deficiency carry one HNPP deletion allele; either *de novo* or inherited. Considering the high frequency of the HNPP susceptibility allele with absence of selection and late adult onset disease (DiVincenzo et al. 2014), it is possible that more novel *COX10* disease alleles can be revealed by sequencing individuals with the HNPP deletion and a mitochondrial spectrum of clinical phenotypes, thereby improving our understanding of the biological function of the *COX10* gene.

The second cohort we assembled is based on the criteria that a patient carries one of the NAHR-deletions and that genotype information of the non-deleted allele is available for analysis. Thus, we selected such individuals from a cohort of 11,091 subjects who were referred for clinical exome sequencing (cES) at a diagnostic laboratory due to a differential clinical diagnosis including various suspected genetic disorders. We performed an initial screen for patients carrying one of the genomic deletions from Table 1, which resulted in 161 subjects carrying one recurrent deletion and 3 subjects carrying two. The two most frequently observed types of deletions, the 15q11.2 BP1−BP2 deletion (n=41) and the *NPHP1*-2q13 deletion (n=23), are excluded from downstream analysis. This is because none of the coding genes from the 15q11.2 BP1−BP2 deletion have been implicated to be associated with Mendelian diseases,(Jonch et al. 2019) and the critical gene at 2q13, *NPHP1*, has been already extensively studied.(Yuan et al. 2015) We also excluded six subjects harboring the X-linked, hemizygous deletion in the Xp22.31 *STS* locus. After excluding these three groups of deletions, exome sequencing data from 95 subjects collectively harboring 96 incidences or 26 types of recurrent genomic deletions were available for us to build the second cohort (Table S7).

This second cohort is not optimized for discovery because it is a collection of various different deletions without any enrichment for a targeted phenotype. Additionally, despite these patients carry one of the disease-associated large deletions, they are still referred to cES analysis; such a property predicts that the disease pathogenesis mechanism found in this cohort tend to be more complex than a typical Mendelian disease cohort, perhaps more likely to represent a ‘blended phenotype’ (Posey et al. 2017). As expected, more than a quarter (26/95) of these subjects were

found to have probable small variant molecular diagnostic findings independent from the deletion. From the remaining 69 subjects with an apparent undiagnostic ES result, we identified 4 subjects with rare variants in coding regions exposed by the deletion as potential molecular diagnoses (Table 3). The first patient is subject #1 described above with HNPP deletion and a *COX10* small variant.

The second patient, subject #3, has clinical features including ataxia, developmental delay, microcephaly, and short stature. A recurrent 10q11.21q11.23 deletion (Stankiewicz et al. 2012) was identified in *trans* with to a novel missense variant c.1490T>C (p.F497S) in the *ERCC6* gene. Biallelic defects in *ERCC6* is associated with cerebro-oculo-facio-skeletal syndrome 1 (COFS1, MIM# 214150) or Cockayne syndrome type B (CSB, MIM# 133540). The high allele frequency of the 10q11.21q11.23 deletion (1.412 $x10^{-4}$) increases the probability for a second allele with ultra-low frequency, like the c.1490T>C (p.F497S) *ERCC6* variant, to be correlated with a set of human clinical phenotypes.

Subject #4 presented with severe neurodevelopmental diseases and dysmorphic features. We identified a hemizygous *OTUD7A* frameshift variant c.2023_2066del (p.D675Hfs*188) in *trans* with the recurrent 15q13.3 BP4-BP5 deletion, providing evidence for *OTUD7A* as a new disease gene. The recurrent deletion mediated by BP4 and BP5 at the 15q13.3 locus is associated with highly variable NDD (neurodevelopmental disorder) phenotypes, ranging from asymptomatic to mild to moderate intellectual disability, epilepsy, behavioral problems, and variable dysmorphic features (Ben-Shachar et al. 2009; van Bon et al. 2009). While heterozygous deletion causes highly variable phenotypes, reported homozygous 15q13.3 BP4-BP5 deletion consistently

manifest disease phenotypes including significant NDD, epilepsy, hypotonia, visual impairments, and other less common phenotypes including autism spectrum disorder, short stature, failure to thrive, microcephaly and variable dysmorphic features (Table S8) (Endris et al. 2010; Lepichon et al. 2010; Masurel-Paulet et al. 2010; Spielmann et al. 2011; Masurel-Paulet et al. 2014). The critical gene responsible for the clinical presentations of the 15q13.3 BP4-BP5 deletion has been debated, but evidence suggests that *OTUD7A*, encoding a member of a family of deubiquitinating enzymes, may be a plausible candidate (Uddin et al. 2018; Yin et al. 2018). Studies using syntenic heterozygous deletion mouse models suggested a critical role of Otud7a in neuronal development and brain function (Uddin et al. 2018; Yin et al. 2018). Otud7a-null mouse models manifest many cardinal features of the 15q13.3 deletion syndrome (Yin et al. 2018). The c.2023_2066del (p.D675Hfs*188) variant identified in subject #4 is located at the last exon of the *OTUD7A* gene, and is thus predicted to not lead to nonsense-mediated decay (NMD) (Coban-Akdemir et al. 2018). However, the variant is predicted to result in substitution of the C-terminal amino acids after aspartic acid with 187 new amino acids and a premature termination of the protein translation (PTC). This change may remove the C-terminal Zinc finger A20-type domain and abolish the normal function of the protein. Our finding in Subject #4, together with recent case reports of patients with a homozygous missense *OTUD7A* variant (Garret et al. 2020) or compound heterozygous 15q13.3 deletion in *trans* with a frameshift *OTUD7A* variant (Suzuki et al. 2020), corroborates that *OTUD7A* may be the critical ‘driver gene’ in the 15q13.3 deletion syndrome, at least in part through a biallelic AR disease trait mechanism. Interestingly, the population small variant allele pool for *OTUD7A* is depleted for LoF alleles based on gnomAD. Without the 15q13.3 deletion contributing to a major carrier burden, the paucity of small variant disease alleles for *OTUD7A* would make disease association establishment using patient data

much more challenging. From an alternative perspective, *OTUD7A*'s current apparent 'high' gene intolerance to haploinsufficiency (pLI=0.95) may have incidentally portraited it as a 'dominant' Mendelian disease gene, whereas its high NIRD score (5.3) of the gene strongly indicate that the intolerance to haploinsufficiency should be much lower, i.e. low likelihood of being a 'dominant' gene.

In Subject #5 with severe neurodevelopmental disorders, we identified a c.649dup (p.R217fs) pathogenic variant in the *PRRT2* gene in *trans* with the recurrent 16p11.2 BP4-BP5 deletion, providing evidence for a novel disease inheritance mechanism for *PRRT2*. The 16p11.2 BP4-BP5 recurrent deletion is known to be associated with mild dysmorphisms, macrocephaly, and neuropsychiatric phenotypes including DD/ID and autism spectrum disorder (ASD) with incomplete penetrance, a NDD (Weiss et al. 2008; Shinawi et al. 2010). The *PRRT2* gene is highly expressed in mouse brain and spinal cord during early embryonic development (Chen et al. 2011). Heterozygous LoF variants in *PRRT2* cause movement and seizure disorders including familial infantile convulsions with paroxysmal choreoathetosis (OMIM# 602066), episodic kinesigenic dyskinesia 1 (EKD1, OMIM# 128200), or benign familial infantile seizures 2 (BFIS2, OMIM# 605751), with incomplete penetrance documented (Meneret et al. 2012). The c.649dup (p.R217fs) allele is the most frequent pathogenic variant, occurring at a mutational hotspot with homopolymer of 9 cytosine bases adjacent to 4 guanine bases that are susceptible to DNA replication errors (Heron et al. 2012). Currently, autosomal dominant (AD) is considered as the only disease inheritance mode for *PRRT2* traits in OMIM, although preliminary evidence from case reports suggest that *PRRT2* can cause a more severe neurodevelopmental disorder through a biallelic pathogenic mechanism and an AR inheritance model (Labate et al. 2012). Our findings

in Subject #5 provide further support for a new disease trait type, AR versus AD, and inheritance mechanism due to *PRRT2* biallelic variation. Moreover, these observations may also pinpoint to a potential model that explains penetrance of certain neurological phenotypes observed in patients with the 16p11.2 deletion; a similar biallelic compound inheritance gene dosage model underlies the penetrance of ~10-12% of congenital scoliosis (Liu et al. 2019a).

NAHR-deletions contribute to recessive disease burden in population-specific patterns

As suggested earlier, the contribution of a given allele to recessive disease burden is influenced by the composition of other pathogenic alleles from the same gene. Although the field is starting to appreciate inter-individual variabilities in NAHR rates associated with alternative genomic structural haplotypes (Shaw-Smith et al. 2006; Yuan et al. 2015) as well as polymorphisms from *trans* acting factors controlling homologous recombination, such as *PRDM9* (Berg et al. 2010), we currently still assume that NAHR mutation rates at a given locus are relatively constant across different ethnic backgrounds. This potentially leaves the remaining alleles, the small variants, as the major driver for any variability in allelic architecture from different population groups. To investigate the degree of inter-population variability for small variant recessive alleles, we used ethnic information from gnomAD, and conducted the modeling described earlier for four population groups, African (AFR), Latino (AMR), East Asian (EAS) and European (EUR) (Table S5). Population specific NIRD scores are compared with the general population to generate ΔNIRD (Figure 3), which can be used to inform the relative odds ratio for NAHR-deletions in recessive disease in the specific population. This analysis provides preliminary computational confirmation for the suspected population variability in NIRD, which implicates that the precision of NIRD can be improved by tuning the model with population specific allelic

architecture. In light of these findings, we tentatively propose that a prioritization strategy based on prior knowledge of population allele frequency spectra can be applied to enhance discovery in research study design of genomic sequencing among individuals with large recurrent deletions. We cautiously note that some of the population groups analyzed here may not have a sufficient sample size to allow a complete representation of disease alleles of relatively lower frequency, which may result in overestimation of ΔNIRD when the score is positive. Additional population specific allele frequency data are warranted to improve the accuracy of this analysis.

Discussion

We cataloged the population frequency spectra of pathogenic alleles across all known recessive diseases. Our analyses highlighted the high frequency of SV mutagenesis and NAHR deletion alleles in genomic instability regions susceptible to this structural rearrangement (Lupski 2007). We subsequently computationally interrogated the impact of allele frequency distributions on recessive disease burden using a modified Punnett square. We used this computational and genetic approach to consider the impact of the NAHR allele on recessive disease traits relative to other recessive variant alleles. Our findings indicate the potentially dramatic disease impact of these NAHR alleles.

Considering current clinical genomics practice and research investigations, we postulate that the role of recurrent genomic deletions and new mutation contributing to recessive diseases is under-appreciated, therefore potentially impeding discovery of new disease genes and alleles. Traditionally, large genomic deletions have been considered to cause dominant disease traits, primarily by a halpoinsufficiency mechanism, with the driver dosage sensitive gene(s) mapping

within the deleted interval. This haploinsufficiency assumption likely arose because these alleles were almost all identified as heterozygotes by screening in symptomatic cohorts and frequently as *de novo* CNV mutations. Our analysis of population frequency implicates that the heterozygous state is often not disease causing, and therefore that these variants act as contributors to recessive disease when they occur in *trans* to a disease allele.

Although many recurrent deletions contribute considerable carrier allele burden to individual recessive Mendelian disease, these deletions are often large enough to include other genes whose homozygous depletions are incompatible with live birth. Two exceptions are the 2q13-*NPHP1* deletion and the *SMN1* deletion (the *SMN1* deletion is predicted by our analysis to be the most frequent NAHR-mediated deletion as shown in Table S1). The fact that other large recurrent deletions are almost never observed in patients as homozygous losses may have led investigators to overlook their equally important role in contributing to recessive disease traits as compound heterozygotes (Boone et al. 2013).

Clinically, there has not been a consensus on whether exome/genome sequencing should be pursued after a recurrent genomic deletion has been identified in a patient. Some may argue that, under the assumption that most Mendelian diseases are caused by one “unifying diagnosis”, the identification of a large genomic deletion can be evidence to demote additional candidate molecular diagnoses in the same patient. Our data argue the opposite: that in patients with a recurrent “contiguous gene deletion syndrome”, the possibility of revealing an “additional” recessive disease molecular diagnosis cannot be ignored.

Coincidentally, four of the five hemizygous small variants exposed by the deletion in Table 3 are located in repeat or difficult-to-sequence regions. The *COX10* and the *PRRT2* frameshift variants were incorrectly called as heterozygous changes by the original exome variant calling pipeline due to challenges of calling indels and mappability issues. If extra care were not taken to look into the deleted hemizygous region, these diagnostic variants would have easily been missed during analysis, which might be one of the reasons contributing to the proposed under-detection of recurrent deletion + small variant cases for recessive disorders.

Of note, the NIRD score devised in this study not only directly depicts the NAHR-deletion contribution to the gene's recessive disease load, but also highlights features not captured by the haploinsufficiency tolerance score pLI. Of the 48 genes with a high NIRD (>3.5) score, 6 have high pLI scores (>0.9) predicting intolerance to haploinsufficiency. These pLI estimations are not accurate because the calculations failed to factor in the population prevalence of NAHR-deletion alleles. Gene level constraint scores should be adjusted particularly for the high NIRD genes.

Taken together, we suggest that the future of new recessive disease and allele discovery will greatly benefit from two approaches: (1) genomic sequencing of individuals with recurrent deletions and (2) sequencing in population of elevated autozygosity (Figure 4). The autozygosity mapping approach has been the classic method for new disease gene discovery in medical genetics. This approach allows a straightforward strategy to target patient populations (by assessing their degree of autozygosity from social and family histories) to assemble the

appropriate cohorts for investigation. However, disease alleles revealed by this approach are usually limited to a specific population.

The NAHR-deletion sequencing approach, on the other hand, has the potential to assign clinical significance to alleles independent of ethnic backgrounds, partly owing to the recurrent and high mutation rate of the NAHR. Nevertheless, this approach requires prior knowledge and screening of individuals for the recurrent deletions. It may have been challenging to collect a cohort of patients with large recurrent deletions two decades ago, but the 'clinical awareness' of genomic disorders, advancements in clinical testing and populational screening have made such a genomic experimental effort feasible, either from large diagnostic centers or from clinical registries (Weiss et al. 2008; Shinawi et al. 2010; Mannik et al. 2015; Dewey et al. 2016; Crawford et al. 2019; Jonch et al. 2019; Edwards et al. 2021). Even when available subject numbers are limited for recurrent genomic deletions with extremely low penetrance, it is possible to tune the disease gene/allele characterization strategy by targeting specific phenotypes, as demonstrated at the Smith Magenis Syndrome - *MYO15* locus two decades ago (Liburd et al. 2001). While researchers are starting to sequence cohorts of individuals with large deletions (Egloff et al. 2018; Beck et al. 2019; Zhao et al. 2020), it is imperative for clinical and diagnostic genomicists to foster guidelines that facilitate routine genomic sequencing (ES or WGS) on patients who are found to have recurrent genomic deletions, which will benefit both the patients and the research enterprises worldwide. Given the great potential in the near future for disease gene discoveries within intervals of genomic deletions, these patients will benefit from routine or perhaps even more prioritized reanalysis of sequencing data (Liu et al. 2019b).

Performing sequencing on personal genomes with higher population prevalence (those from Table 1) carries additional long-term promise for clinical characterization of common variants, extending the current scope of focus on mono- or bi- allelic inheritance into the more complex spectrum of disease inheritance – including the compound inheritance gene dosage model (Wu et al. 2015). High prevalence recurrent genomic deletions are often associated with a high degree of incomplete penetrance of disease phenotype, ranging from 10-90% (Rosenfeld et al. 2013). The disease causal mechanism described in this study, for example, the 16p11.2 deletion + the *PRRT2* small variant leading to NDD, may explain a small portion of the previously-attributed missing heritability for the disease "penetrance" at 16p11.2. However, the totality of the missing heritability is likely not explained by the recessive model alone, because the observed disease penetrance is likely to dominate the aggregation of the recessive disease allele prevalence (individually rare) on the non-deleted chromosome. It is plausible that alternative disease models exist, in which the critical gene triggers disease presentation when one rare LoF allele is combined with one or a set of milder hypomorphic alleles with common population frequency. This compound inheritance model has been demonstrated at the *RBM8A*-1q21.1 locus in association with the TAR syndrome (Albers et al. 2012), the *TBX6*-16p11.2 locus in association with congenital scoliosis (Wu et al. 2015), and the *F12*-5q35 Sotos deletion locus in association with blood clotting (Kurotaki et al. 2005). Our analysis in this study was focused on coding sequence changes. Moreover, the limited size of patient cohort ascertained for each recurrent deletion may decrease the power of identifying high frequency hypomorphic alleles. These will be dramatically empowered by genome sequencing in a larger patient cohort. Nevertheless, the unifying theme for both the strictly recessive model and the more complex compound inheritance gene dosage model is that large recurrent genomic deletions provide a unique

perspective in characterization of new disease loci and alleles and the emerging field of human haploid genetics.

Methods

Construction of a genome-wide map for NAHR-mediated recurrent genomic deletions

Hotspots of recurrent deletions were characterized with overlapping intervals flanked by clustering SD pairs, which illustrates that distinctive mechanistic events can contribute to each of the same clinically recognized genomic disorders. SD pairs, for which intervening genomic segments are likely to be clinically interpreted as the same genomic deletion, were collapsed. Metrics that could inform estimation of the new mutation rates for each genomic disorder were kept for each SD elements from the merged cluster of repeats, including repeat lengths, distance in between, and sequence similarity (Liu et al. 2011). Gene content of the deleted segment is expected to influence the fitness of this allele. We used the number of genes with a high pLI score, i.e. greater intolerant to haploinsufficiency, to estimate the level of selection to the genomic deletion in the population. These metrics were used to calculate a score to estimate the relative populational prevalence of these CNVs. Coordinates for deletion breakpoints are calculated as a weighted average of all the ranges of possible SDs that may mediate the deletion. Thus, the coordinates are not precise predictions for a specific deletion observed in individual patients, but rather average of all possible types of deletions that were collapsed into the merged deletion. Two separate NAHR-deletion maps were generated using SegDup tracks from GRCh38 and GRCh37.

Prevalence curation for NAHR-mediated recurrent genomic deletions

For genomic deletions with a population prevalence over 1/1,000,000, prevalence estimates were calculated based on the UK Biobank cohort (Crawford et al. 2019) and the Icelandic cohort (Stefansson et al. 2014). If the prevalence estimate was not significantly different between these cohorts (Fisher's exact test, $p>0.05$), the estimate based on the UK Biobank data was taken. Otherwise, prevalence from a third cohort [gnomAD SV (Collins et al. 2020) or other region specific literature] was compared with estimates from the UK Biobank and the Icelandic cohorts, and the group with a closer match was taken. For genomic deletions with a prevalence lower than 1/1,000,000, we investigated a cohort of 33,452 patients who were referred for clinical Chromosomal Microarray Analysis (CMA) using custom designed Agilent oligo-based Comparative Genomic Hybridization arrays (Yuan et al. 2020). Of note, deletion prevalence estimates from the CMA cohort do not represent actual prevalences in the general population, but can inform relative prevalence comparison among rare events in the population.

Recessive disease carrier burden calculation

High-quality ClinVar variants were defined as having a pathogenic or likely pathogenic label with at least one-star review status (accessed 01/21/2021). LoF variants from gnomAD SV were defined by variants meeting all the following criteria (1) PASS filter in the VCF file with a quality score over 500, (2) PROTEIN_CODING__LOF flag or PROTEIN_CODING__DUP_LOF flag in the VCF file, (3) POPMAX allele frequency lower than 1% and no homozygote counts, (4) less than 80% of the span overlapping with segmental duplications, and (6) the LoF consequence affects all RefSeq transcripts of a recessive gene. High-confidence LoF small variants from gnomAD v3.1 were defined by variants that fulfill all the following criteria: (1) PASS filter from the gnomAD v3.1 VCF file, (2) do not fall into a low

complexity region, (3) QUALapprox score lower than $1x10^5$, (4) sequenced in over $7.5x10^4$ alleles, (5) population allele frequency lower than 1% with no homozygous counts, and (6) marked as a high-quality LoF variant by LOFTEE (Karczewski et al. 2020).

Calculation of NAHR-deletion contribution to disease burden for a specific recessive disorder

All the following calculations are based on the concept of random mating by sampling from a pool of alleles. Suppose, that at an autosomal recessive locus, we have *n* alleles, A_1, A_2, … A_n, with allele frequencies p_1, p_2, p_3, …, p_n. Without loss of generality, we nominate the kth allele as the NAHR-deletion allele -our allele of interest - and let the others index the small variant alleles. For most large recurrent deletions, homozygous loss of the deletion is incompatible with live birth. The two exceptions are the 2q13-*NPHP1* deletion and the 15q13.3 BP4-BP5 deletion, for which homozygous deletions are compatible with live birth. Also, the 15q13.3 BP4-BP5 deletion is encompassed by the 15q11q13 BP3-BP5 deletion, so the enclosed recessive genes have two NAHR-deletions contributing to them. Hypomorphic alleles that cause disease when they co-occur with LoF alleles, which we denote as A_h, are not disease-causing in homozygous states. Such alleles are observed in *RBM8A* and *TBX6*, but at present not in others. The exceptions described above regarding *RBM8A*, *TBX6*, the 2q13-*NPHP1* deletion, and the 15q13.3 BP4-BP5 deletion have been accounted for in the calculations for these special circumstances. For simplicity, they are not incorporated in the equations below, although the modifications to account for them are simple adjustments to the sums and formulate presented below.

We denote the probability of an individual carrying the NAHR-deletion allele is

$$P\left(A_k\right) = p_k$$

The contribution of the NAHR-deletion to the allele load (**Fa**) is the fraction of the NAHR-deletion allele frequency over the sum of all allele frequencies across all functional alleles - except for the hypomophric alleles that do not in themselves cause disease.

$$Fa_k = \frac{p_k}{\sum_{i=1}^{n} p_i}$$

The Punnett square below models the expected frequencies of an individual to be affected with the recessive trait given the population frequencies of each pair of alleles under a random mating model.

	A_1 p_1	A_2 p_2	…	A_k p_k	…	A_n p_n
A_1 p_1	p_1^2 A_1A_1	p_1p_2 A_1A_2	…	p_1p_k A_1A_k	…	p_1p_n A_1A_n
A_2 p_2	p_1p_2 A_1A_2	p_2^2 A_2A_2	…	p_2p_k A_2A_k	…	p_2p_n A_2A_n
⋮	⋮	⋮	…	…	…	…
A_k p_k	p_1p_k A_1A_k	p_2p_k A_2A_k	…	p_k^2 A_kA_k	…	p_kp_n A_kA_n
⋮	⋮	⋮	…	⋮	…	…
A_n p_n	p_1p_n A_1A_n	p_2p_n A_2A_n	…	p_kp_n A_kA_n	…	p_n^2 A_nA_n

The probability for an individual to be affected with the recessive disorder is the sum of pairwise products of all carrier alleles with contribution from the homozygous NAHR-deletion lethal allele subtracted

$$P\left(D\right) = \sum_{i=1}^{n}\sum_{j=1}^{n} p_i p_j - p_k^2$$

The probability for an individual to be both affected with the recessive disorder and carrying the NAHR-deletion is

$$P\left(A_k \cap D\right) = 2 \cdot \sum_{j=1}^{n} p_k p_j - 2 \cdot p_k^2$$

The contribution of individuals with the NAHR-deletion to the recessive disease load (**Fd**) is

$$Fd_k = P\left(A_k | D\right) = \frac{P\left(A_k \cap D\right)}{P\left(D\right)}$$

The odds for an individual with the recessive disease to carry the NAHR deletion is

$$O_k = \frac{Fd_k}{\sum_{i=1}^{n} Fd_i - Fd_k}$$

Note that the sum of Fd across alleles *1, 2, 3, …, n* equals the sum of the Punnett square matrix plus the lower triangular and the upper triangular. This is equivalent to summing up homozygous allele products once plus compound heterozygous allele products twice. This characteristic arises because the events of recessive disease involving the kth and the jth allele are not disjoint and they overlap for the compound heterozygote entries in the Punnett square.

To calculate the NAHR-deletion Impact to Recessive Disease score, the odds of the NAHR allele is compared to that of the "median" allele from the same gene.

$$NIRD = \log_2\left(OR_k\right) = \log_2\left(\frac{O_k}{O_{median}}\right)$$

The "median" allele is defined as the midpoint of remaining alleles in the same gene that comprise a cumulative sum of the top 90% of the overall sum of Fd. The alleles consisting the

lower 10% of overall Fd sum are disregarded because (1) we find many genes have a long tail of ultra-rare alleles without a frequency estimate from gnomAD, and (2) we supplemented 10% of hypothetical alleles to each gene in our analysis.

Curation of recessive disease alleles from the meta-analysis of the 170 patients identified from the literature

The Human Gene Mutation Database (HGMD, version 2020.4) was queried for recessive disease alleles in genes for which ≥70% of the disease carrier burden was attributed to NAHR-mediated large deletions. The literature linked to each disease allele that was marked as a disease-causing mutation (DM) or possible DM (DM?) was mined for the allelic state of the variant (homozygous, compound heterozygous with another SNV, or compound heterozygous with the NAHR-mediated deletion) as well as the number of unrelated families carrying the allele. Homozygous variants were counted once per family, while compound heterozygous SNVs received one count each per family. Gross deletions and insertions larger than 50 bp were excluded. *RBM8A* was the only gene for which disease-associated polymorphisms with additional supporting functional evidence (DFP) were also included; DM/DM? alleles compound heterozygous with DFP variants were dismissed for all genes other than *RBM8A*. *MYH11* and *PMP22* are the only two genes in this curation effort to have disease associations of both autosomal dominant and recessive inheritance. *MYH11* alleles were only added if they were associated with hypoperistalsis. Similarly, only biallelic loss-of-function *PMP22* alleles were included. The total population frequency of each curated allele was retrieved using gnomAD v3.1.

Retrospective analysis of extant cES for new recessive gene and allele discovery from individuals with recurrent genomic deletions

This study has been performed in accordance with the research protocol approved by Institutional Review Boards at Baylor College of Medicine. A waiver of informed consent has been obtained (H-41191). The patients were evaluated by clinical exome sequencing, with sequencing, data analysis, and interpretation procedures described previously (Yang et al. 2013; Yang et al. 2014). The identification of deletions was based on a SNP array platform, which was performed concurrently with the exome assay (Dharmadhikari et al. 2019). Sanger sequencing was performed as a validation method for candidate diagnostic small variants.

Code availability

Detailed code for generation of the NAHR-deletion map, preparation of disease alleles, and calculation of disease burden is available at https://github.com/liu-lab/cnvNAHR/.

References

Albers CA, Paul DS, Schulze H, Freson K, Stephens JC, Smethurst PA, Jolley JD, Cvejic A, Kostadima M, Bertone P et al. 2012. Compound inheritance of a low-frequency regulatory SNP and a rare null mutation in exon-junction complex subunit *RBM8A* causes TAR syndrome. *Nat Genet* **44**: 435-439, S431-432.

Alkuraya FS. 2021. A genetic revolution in rare-disease medicine. *Nature* **590**: 218-219.

Bamshad MJ, Nickerson DA, Chong JX. 2019. Mendelian Gene Discovery: Fast and Furious with No End in Sight. *Am J Hum Genet* **105**: 448-455.

Beck CR, Carvalho CMB, Akdemir ZC, Sedlazeck FJ, Song X, Meng Q, Hu J, Doddapaneni H, Chong Z, Chen ES et al. 2019. Megabase Length Hypermutation Accompanies Human Structural Variation at 17p11.2. *Cell* **176**: 1310-1324 e1310.

Ben-Shachar S, Lanpher B, German JR, Qasaymeh M, Potocki L, Nagamani SC, Franco LM, Malphrus A, Bottenfield GW, Spence JE et al. 2009. Microdeletion 15q13.3: a locus with incomplete penetrance for autism, mental retardation, and psychiatric disorders. *J Med Genet* **46**: 382-388.

Berg IL, Neumann R, Lam KW, Sarbajna S, Odenthal-Hesse L, May CA, Jeffreys AJ. 2010. *PRDM9* variation strongly influences recombination hot-spot activity and meiotic instability in humans. *Nat Genet* **42**: 859-863.

Boone PM, Campbell IM, Baggett BC, Soens ZT, Rao MM, Hixson PM, Patel A, Bi W, Cheung SW, Lalani SR et al. 2013. Deletions of recessive disease genes: CNV contribution to carrier states and disease-causing alleles. *Genome Res* **23**: 1383-1394.

Cacheiro P, Munoz-Fuentes V, Murray SA, Dickinson ME, Bucan M, Nutter LMJ, Peterson KA, Haselimashhadi H, Flenniken AM, Morgan H et al. 2020. Human and mouse essentiality screens as a resource for disease gene discovery. *Nature communications* **11**: 655.

Chen WJ, Lin Y, Xiong ZQ, Wei W, Ni W, Tan GH, Guo SL, He J, Chen YF, Zhang QJ et al. 2011. Exome sequencing identifies truncating mutations in *PRRT2* that cause paroxysmal kinesigenic dyskinesia. *Nat Genet* **43**: 1252-1255.

Coban-Akdemir Z, Song X, Pehlivan D, Karaca E, Bayram Y, Gambin T, Jhangiani SN, Muzny DM, Lewis RA, Baylor Hopkins Center for Mendelian Genomics et al. 2020. De novo mutation in ancestral generations evolves haplotypes contributing to disease. *bioRxiv* **https://doi.org/10.1101/2020.04.27.064824**.

Coban-Akdemir Z, White JJ, Song X, Jhangiani SN, Fatih JM, Gambin T, Bayram Y, Chinn IK, Karaca E, Punetha J et al. 2018. Identifying Genes Whose Mutant Transcripts Cause Dominant Disease Traits by Potential Gain-of-Function Alleles. *Am J Hum Genet* **103**: 171-187.

Coleman MP, Conforti L, Buckmaster EA, Tarlton A, Ewing RM, Brown MC, Lyon MF, Perry VH. 1998. An 85-kb tandem triplication in the slow Wallerian degeneration (Wlds) mouse. *Proc Natl Acad Sci U S A* **95**: 9985-9990.

Collins RL, Brand H, Karczewski KJ, Zhao X, Alfoldi J, Francioli LC, Khera AV, Lowther C, Gauthier LD, Wang H et al. 2020. A structural variation reference for medical and population genetics. *Nature* **581**: 444-451.

Crawford K, Bracher-Smith M, Owen D, Kendall KM, Rees E, Pardinas AF, Einon M, Escott-Price V, Walters JTR, O'Donovan MC et al. 2019. Medical consequences of pathogenic CNVs in adults: analysis of the UK Biobank. *J Med Genet* **56**: 131-138.

Dennis MY, Eichler EE. 2016. Human adaptation and evolution by segmental duplication. *Current opinion in genetics & development* **41**: 44-52.

Dewey FE, Murray MF, Overton JD, Habegger L, Leader JB, Fetterolf SN, O'Dushlaine C, Van Hout CV, Staples J, Gonzaga-Jauregui C et al. 2016. Distribution and clinical impact of functional variants in 50,726 whole-exome sequences from the DiscovEHR study. *Science* **354**.

Dharmadhikari AV, Ghosh R, Yuan B, Liu P, Dai H, Al Masri S, Scull J, Posey JE, Jiang AH, He W et al. 2019. Copy number variant and runs of homozygosity detection by microarrays enabled more precise molecular diagnoses in 11,020 clinical exome cases. *Genome Med* **11**: 30.

Dittwald P, Gambin T, Szafranski P, Li J, Amato S, Divon MY, Rodriguez Rojas LX, Elton LE, Scott DA, Schaaf CP et al. 2013. NAHR-mediated copy-number variants in a clinical population: Mechanistic insights into both genomic disorders and Mendelizing traits. *Genome Res* **23**: 1395-1409.

DiVincenzo C, Elzinga CD, Medeiros AC, Karbassi I, Jones JR, Evans MC, Braastad CD, Bishop CM, Jaremko M, Wang Z et al. 2014. The allelic spectrum of Charcot-Marie-Tooth disease in over 17,000 individuals with neuropathy. *Mol Genet Genomic Med* **2**: 522-529.

Edwards SD, Schulze KV, Rosenfeld JA, Westerfield LE, Gerard A, Yuan B, Grigorenko EL, Posey JE, Bi W, Liu P. 2021. Clinical characterization of individuals with the distal 1q21.1 microdeletion. *Am J Med Genet A* doi:10.1002/ajmg.a.62104.

Egloff M, Nguyen LS, Siquier-Pernet K, Cormier-Daire V, Baujat G, Attie-Bitach T, Bole-Feysot C, Nitschke P, Vekemans M, Colleaux L et al. 2018. Whole-exome sequence

analysis highlights the role of unmasked recessive mutations in copy number variants with incomplete penetrance. *Eur J Hum Genet* **26**: 912-918.

Endris V, Hackmann K, Neuhann TM, Grasshoff U, Bonin M, Haug U, Hahn G, Schallner JC, Schrock E, Tinschert S et al. 2010. Homozygous loss of CHRNA7 on chromosome 15q13.3 causes severe encephalopathy with seizures and hypotonia. *Am J Med Genet A* **152A**: 2908-2911.

Garret P, Ebstein F, Delplancq G, Dozieres-Puyravel B, Boughalem A, Auvin S, Duffourd Y, Klafack S, Zieba BA, Mahmoudi S et al. 2020. Report of the first patient with a homozygous *OTUD7A* variant responsible for epileptic encephalopathy and related proteasome dysfunction. *Clin Genet* **97**: 567-575.

Gonzaga-Jauregui C, Yesil G, Nistala H, Gezdirici A, Bayram Y, Nannuru KC, Pehlivan D, Yuan B, Jimenez J, Sahin Y et al. 2020. Functional biology of the Steel syndrome founder allele and evidence for clan genomics derivation of *COL27A1* pathogenic alleles worldwide. *Eur J Hum Genet* **28**: 1243-1264.

Haque IS, Lazarin GA, Kang HP, Evans EA, Goldberg JD, Wapner RJ. 2016. Modeled Fetal Risk of Genetic Diseases Identified by Expanded Carrier Screening. *Jama* **316**: 734-742.

Heron SE, Grinton BE, Kivity S, Afawi Z, Zuberi SM, Hughes JN, Pridmore C, Hodgson BL, Iona X, Sadleir LG et al. 2012. *PRRT2* mutations cause benign familial infantile epilepsy and infantile convulsions with choreoathetosis syndrome. *Am J Hum Genet* **90**: 152-160.

Jonch AE, Douard E, Moreau C, Van Dijck A, Passeggeri M, Kooy F, Puechberty J, Campbell C, Sanlaville D, Lefroy H et al. 2019. Estimating the effect size of the 15q11.2 BP1-BP2 deletion and its contribution to neurodevelopmental symptoms: recommendations for practice. *J Med Genet* **56**: 701-710.

Karczewski KJ, Francioli LC, Tiao G, Cummings BB, Alfoldi J, Wang Q, Collins RL, Laricchia KM, Ganna A, Birnbaum DP et al. 2020. The mutational constraint spectrum quantified from variation in 141,456 humans. *Nature* **581**: 434-443.

Klopocki E, Schulze H, Strauss G, Ott CE, Hall J, Trotier F, Fleischhauer S, Greenhalgh L, Newbury-Ecob RA, Neumann LM et al. 2007. Complex inheritance pattern resembling autosomal recessive inheritance involving a microdeletion in thrombocytopenia-absent radius syndrome. *Am J Hum Genet* **80**: 232-240.

Kurotaki N, Shen JJ, Touyama M, Kondoh T, Visser R, Ozaki T, Nishimoto J, Shiihara T, Uetake K, Makita Y et al. 2005. Phenotypic consequences of genetic variation at hemizygous alleles: Sotos syndrome is a contiguous gene syndrome incorporating coagulation factor twelve (*FXII*) deficiency. *Genet Med* **7**: 479-483.

Labate A, Tarantino P, Viri M, Mumoli L, Gagliardi M, Romeo A, Zara F, Annesi G, Gambardella A. 2012. Homozygous c.649dupC mutation in *PRRT2* worsens the BFIS/PKD phenotype with mental retardation, episodic ataxia, and absences. *Epilepsia* **53**: e196-199.

Lepichon JB, Bittel DC, Graf WD, Yu S. 2010. A 15q13.3 homozygous microdeletion associated with a severe neurodevelopmental disorder suggests putative functions of the *TRPM1*, *CHRNA7*, and other homozygously deleted genes. *Am J Med Genet A* **152A**: 1300-1304.

Liburd N, Ghosh M, Riazuddin S, Naz S, Khan S, Ahmed Z, Riazuddin S, Liang Y, Menon PS, Smith T et al. 2001. Novel mutations of *MYO15A* associated with profound deafness in consanguineous families and moderately severe hearing loss in a patient with Smith-Magenis syndrome. *Hum Genet* **109**: 535-541.

Liu J, Wu N, Deciphering Disorders Involving S, study CO, Yang N, Takeda K, Chen W, Li W, Du R, Liu S et al. 2019a. *TBX6*-associated congenital scoliosis (TACS) as a clinically distinguishable subtype of congenital scoliosis: further evidence supporting the compound inheritance and *TBX6* gene dosage model. *Genet Med* **21**: 1548-1558.

Liu P, Carvalho CM, Hastings PJ, Lupski JR. 2012. Mechanisms for recurrent and complex human genomic rearrangements. *Current opinion in genetics & development* **22**: 211-220.

Liu P, Lacaria M, Zhang F, Withers M, Hastings PJ, Lupski JR. 2011. Frequency of Nonallelic Homologous Recombination Is Correlated with Length of Homology: Evidence that Ectopic Synapsis Precedes Ectopic Crossing-Over. *Am J Hum Genet* **89**: 580-588.

Liu P, Meng L, Normand EA, Xia F, Song X, Ghazi A, Rosenfeld J, Magoulas PL, Braxton A, Ward P et al. 2019b. Reanalysis of Clinical Exome Sequencing Data. *N Engl J Med* **380**: 2478-2480.

Lupski JR. 2007. Genomic rearrangements and sporadic disease. *Nat Genet* **39**: S43-47.

Lupski JR. 2015a. Cognitive phenotypes and genomic copy number variations. *Jama* **313**: 2029-2030.

Lupski JR. 2015b. Structural variation mutagenesis of the human genome: Impact on disease and evolution. *Environmental and molecular mutagenesis* **56**: 419-436.

Lupski JR. 2019. 2018 Victor A. McKusick Leadership Award: Molecular Mechanisms for Genomic and Chromosomal Rearrangements. *Am J Hum Genet* **104**: 391-406.

Lupski JR. 2021. Clan genomics: From OMIM phenotypic traits to genes and biology. *Am J Med Genet A* **185**: 3294-3313.

Lupski JR, Belmont JW, Boerwinkle E, Gibbs RA. 2011. Clan genomics and the complex architecture of human disease. *Cell* **147**: 32-43.

Mannik K, Magi R, Mace A, Cole B, Guyatt AL, Shihab HA, Maillard AM, Alavere H, Kolk A, Reigo A et al. 2015. Copy number variations and cognitive phenotypes in unselected populations. *Jama* **313**: 2044-2054.

Martin HC, Jones WD, McIntyre R, Sanchez-Andrade G, Sanderson M, Stephenson JD, Jones CP, Handsaker J, Gallone G, Bruntraeger M et al. 2018. Quantifying the contribution of recessive coding variation to developmental disorders. *Science* **362**: 1161-1164.

Masurel-Paulet A, Andrieux J, Callier P, Cuisset JM, Le Caignec C, Holder M, Thauvin-Robinet C, Doray B, Flori E, Alex-Cordier MP et al. 2010. Delineation of 15q13.3 microdeletions. *Clin Genet* **78**: 149-161.

Masurel-Paulet A, Drumare I, Holder M, Cuisset JM, Vallee L, Defoort S, Bourgois B, Pernes P, Cuvellier JC, Huet F et al. 2014. Further delineation of eye manifestations in homozygous 15q13.3 microdeletions including *TRPM1*: a differential diagnosis of ceroid lipofuscinosis. *Am J Med Genet A* **164A**: 1537-1544.

Meneret A, Grabli D, Depienne C, Gaudebout C, Picard F, Durr A, Lagroua I, Bouteiller D, Mignot C, Doummar D et al. 2012. *PRRT2* mutations: a major cause of paroxysmal kinesigenic dyskinesia in the European population. *Neurology* **79**: 170-174.

Posey JE, Harel T, Liu P, Rosenfeld JA, James RA, Coban Akdemir ZH, Walkiewicz M, Bi W, Xiao R, Ding Y et al. 2017. Resolution of Disease Phenotypes Resulting from Multilocus Genomic Variation. *N Engl J Med* **376**: 21-31.

Posey JE, O'Donnell-Luria AH, Chong JX, Harel T, Jhangiani SN, Coban Akdemir ZH, Buyske S, Pehlivan D, Carvalho CMB, Baxter S et al. 2019. Insights into genetics, human biology and disease gleaned from family based genomic studies. *Genet Med* **21**: 798-812.

Potocki L, Chen KS, Koeuth T, Killian J, Iannaccone ST, Shapira SK, Kashork CD, Spikes AS, Shaffer LG, Lupski JR. 1999. DNA rearrangements on both homologues of chromosome 17 in a mildly delayed individual with a family history of autosomal dominant carpal tunnel syndrome. *Am J Hum Genet* **64**: 471-478.

Ren X, Yang N, Wu N, Xu X, Chen W, Zhang L, Li Y, Du RQ, Dong S, Zhao S et al. 2020. Increased *TBX6* gene dosages induce congenital cervical vertebral malformations in humans and mice. *J Med Genet* **57**: 371-379.

Rosenfeld JA, Coe BP, Eichler EE, Cuckle H, Shaffer LG. 2013. Estimates of penetrance for recurrent pathogenic copy-number variations. *Genet Med* **15**: 478-481.

Shaw-Smith C, Pittman AM, Willatt L, Martin H, Rickman L, Gribble S, Curley R, Cumming S, Dunn C, Kalaitzopoulos D et al. 2006. Microdeletion encompassing *MAPT* at chromosome 17q21.3 is associated with developmental delay and learning disability. *Nat Genet* **38**: 1032-1037.

Shinawi M, Liu P, Kang SH, Shen J, Belmont JW, Scott DA, Probst FJ, Craigen WJ, Graham BH, Pursley A et al. 2010. Recurrent reciprocal 16p11.2 rearrangements associated with global developmental delay, behavioural problems, dysmorphism, epilepsy, and abnormal head size. *J Med Genet* **47**: 332-341.

Spielmann M, Reichelt G, Hertzberg C, Trimborn M, Mundlos S, Horn D, Klopocki E. 2011. Homozygous deletion of chromosome 15q13.3 including *CHRNA7* causes severe mental retardation, seizures, muscular hypotonia, and the loss of *KLF13* and *TRPM1* potentially

cause macrocytosis and congenital retinal dysfunction in siblings. *Eur J Med Genet* **54**: e441-445.

Stankiewicz P, Kulkarni S, Dharmadhikari AV, Sampath S, Bhatt SS, Shaikh TH, Xia Z, Pursley AN, Cooper ML, Shinawi M et al. 2012. Recurrent deletions and reciprocal duplications of 10q11.21q11.23 including *CHAT* and *SLC18A3* are likely mediated by complex low-copy repeats. *Hum Mutat* **33**: 165-179.

Stefansson H, Meyer-Lindenberg A, Steinberg S, Magnusdottir B, Morgen K, Arnarsdottir S, Bjornsdottir G, Walters GB, Jonsdottir GA, Doyle OM et al. 2014. CNVs conferring risk of autism or schizophrenia affect cognition in controls. *Nature* **505**: 361-366.

Suzuki H, Inaba M, Yamada M, Uehara T, Takenouchi T, Mizuno S, Kosaki K, Doi M. 2020. Biallelic loss of *OTUD7A* causes severe muscular hypotonia, intellectual disability, and seizures. *Am J Med Genet A* doi:10.1002/ajmg.a.62054.

Turner DJ, Miretti M, Rajan D, Fiegler H, Carter NP, Blayney ML, Beck S, Hurles ME. 2008. Germline rates of de novo meiotic deletions and duplications causing several genomic disorders. *Nat Genet* **40**: 90-95.

Tyson J, Malcolm S, Thomas PK, Harding AE. 1996. Deletions of chromosome 17p11.2 in multifocal neuropathies. *Ann Neurol* **39**: 180-186.

Uddin M, Unda BK, Kwan V, Holzapfel NT, White SH, Chalil L, Woodbury-Smith M, Ho KS, Harward E, Murtaza N et al. 2018. *OTUD7A* Regulates Neurodevelopmental Phenotypes in the 15q13.3 Microdeletion Syndrome. *Am J Hum Genet* **102**: 278-295.

van Bon BW, Mefford HC, Menten B, Koolen DA, Sharp AJ, Nillesen WM, Innis JW, de Ravel TJ, Mercer CL, Fichera M et al. 2009. Further delineation of the 15q13 microdeletion and

duplication syndromes: a clinical spectrum varying from non-pathogenic to a severe outcome. *J Med Genet* **46**: 511-523.

Weiss LA, Shen Y, Korn JM, Arking DE, Miller DT, Fossdal R, Saemundsen E, Stefansson H, Ferreira MA, Green T et al. 2008. Association between microdeletion and microduplication at 16p11.2 and autism. *N Engl J Med* **358**: 667-675.

Wu N, Ming X, Xiao J, Wu Z, Chen X, Shinawi M, Shen Y, Yu G, Liu J, Xie H et al. 2015. *TBX6* null variants and a common hypomorphic allele in congenital scoliosis. *N Engl J Med* **372**: 341-350.

Yang N, Wu N, Zhang L, Zhao Y, Liu J, Liang X, Ren X, Li W, Chen W, Dong S et al. 2019. *TBX6* compound inheritance leads to congenital vertebral malformations in humans and mice. *Hum Mol Genet* **28**: 539-547.

Yang Y, Muzny DM, Reid JG, Bainbridge MN, Willis A, Ward PA, Braxton A, Beuten J, Xia F, Niu Z et al. 2013. Clinical whole-exome sequencing for the diagnosis of mendelian disorders. *N Engl J Med* **369**: 1502-1511.

Yang Y, Muzny DM, Xia F, Niu Z, Person R, Ding Y, Ward P, Braxton A, Wang M, Buhay C et al. 2014. Molecular findings among patients referred for clinical whole-exome sequencing. *Jama* **312**: 1870-1879.

Yin J, Chen W, Chao ES, Soriano S, Wang L, Wang W, Cummock SE, Tao H, Pang K, Liu Z et al. 2018. Otud7a Knockout Mice Recapitulate Many Neurological Features of 15q13.3 Microdeletion Syndrome. *Am J Hum Genet* **102**: 296-308.

Yuan B, Liu P, Gupta A, Beck CR, Tejomurtula A, Campbell IM, Gambin T, Simmons AD, Withers MA, Harris RA et al. 2015. Comparative Genomic Analyses of the Human

NPHP1 Locus Reveal Complex Genomic Architecture and Its Regional Evolution in Primates. *PLoS Genet* **11**: e1005686.

Yuan B, Wang L, Liu P, Shaw C, Dai H, Cooper L, Zhu W, Anderson SA, Meng L, Wang X et al. 2020. CNVs cause autosomal recessive genetic diseases with or without involvement of SNV/indels. *Genet Med* **22**: 1633-1641.

Zhao Y, Diacou A, Johnston HR, Musfee FI, McDonald-McGinn DM, McGinn D, Crowley TB, Repetto GM, Swillen A, Breckpot J et al. 2020. Complete Sequence of the 22q11.2 Allele in 1,053 Subjects with 22q11.2 Deletion Syndrome Reveals Modifiers of Conotruncal Heart Defects. *Am J Hum Genet* **106**: 26-40.

Declaration of interests

Baylor College of Medicine (BCM) and Miraca Holdings Inc. have formed a joint venture with shared ownership and governance of Baylor Genetics (BG), which performs clinical exome sequencing and chromosomal microarray genomics assay services. The authors who are affiliated with BG are employees of BCM and derive support through a professional services agreement with the BG. JRL has stock ownership in 23andMe, is a paid consultant for Regeneron Pharmaceuticals and Novartis, and is a co-inventor on multiple United States and European patents related to molecular diagnostics for inherited neuropathies, eye diseases, and bacterial genomic fingerprinting.

ACKNOWLEDGMENTS

This work was supported by the National Human Genome Research Institute (NHGRI) grant number R35HG011311 to PL, Baylor College of Medicine Precision Medicine Initiative Pilot Award to PL, National Human Genome Research Institute (NHGRI)/ National Heart Lung and Blood Institute (NHLBI) grant number UM1HG006542 to the Baylor Hopkins Center for Mendelian Genomics (BHCMG) to JRL, the National Institute of Neurological Disorders and Stroke (NINDS) R35NS105078 to JRL.

.

Tables and Figures

Table 1. Recurrent genomic deletions that are prevalent in the population.

Region	Coordinates (GRCh38)	Population allele frequency (x 10^{-6})	Allele frequency in diagnostic testing (x 10^{-6})	Known recessive genes	Number of coding genes
2q13 *NPHP1*	chr2:109930242-110228182	5873	2616	*NPHP1*	3
15q11.2	chr15:21311962-23261294	2764	2287	-	14
16p12.1	chr16:21754781-22502804	592.3	627.8	*OTOA, UQCRC2*	11
17p12 HNPP	chr17:14170711-15567588	314.8	388.6	*COX10, PMP22*	9
16p13.11	chr16:14772948-16330433	312.6	433.5	*NDE1, MYH11, ABCC6*	15
1q21.1 BP3-BP4	chr1:146380249-148811725	267.2	672.6	-	15
16p11.2 proximal	chr16:29416551-30202090	259.6	1674	*PRRT2, ALDOA, TBX6, CORO1A*	35
13q12.12	chr13:22911590-24323812	211.7	104.6	*SGCG, SACS, MIPEP*	7
22q11.2 LCRA-D	chr22:18530098-21214537	177.1	4499	*PRODH, SLC25A1, CDC45, GP1BB, TXNRD2, TANGO2, SCARF2, PI4KA, SNAP29, LZTR1*	49
1q21 TAR	chr1:144904297-146209950	173.9	269.0	*PEX11B, RBM8A, POLR3GL, HJV*	22

10q11.21q11.23	chr10:45765081-49954967	141.2	74.73	*RBP3, ERCC6, SLC18A3, CHAT*	38
16p11.2 distal	chr16:28706949-29049993	136.1	254.1	*TUFM, ATP2A1, CD19, LAT*	11
2q13	chr2:110494056-112385043	128.6	149.5	*ANAPC1, MERTK*	11
2q21.1	chr2:130623447-131386379	100.8	119.6	-	9
15q13.3 BP4-BP5	chr15:30246847-32496522	93.26	896.8	*FAN1, TRPM1, OTUD7A*	13
2q11.2	chr2:95759114-97430329	73.10	74.73	*ADRA2B, NCAPH, LMAN2L, CNNM4*	24
17q12	chr17:36300613-38034442	68.86	463.4	*ZNHIT3, PIGW*	21
7q11.23	chr7:73089294-74862006	39.35	1375	*NCF1*	27
15q11q13 BP3-BP4	chr15:28580349-30417865	35.29	134.5	*NSMCE3*	10
3q29	chr3:195963652-197626678	22.69	194.3	*TFRC, PCYT1A, TCTEX1D2, RNF168, NRROS, CEP19*	23
17q11.2	chr17:30621877-32037969	22.66	149.5	-	14
22q11.2 LCRD-H	chr22:21206521-24255497	12.60	59.79	*IGLL1*	45
8p23.1	chr8:7596999-12344083	10.08	134.5	*RP1L1, FDFT1*	50
10q23	chr10:79733715-87254783	7.562	59.79	*MAT1A, CDHR1*	31
17p11.2 Smith Magenis Syndrome	chr17:16777950-20450859	5.041	687.6	*TNFRSF13B, ATPAF2, MYO15A, MEIF2, TOP3A, GRAP, B9D1, ALDH3A2*	48
15q11 Prader-Willi/	chr15:21976318-	2.521	687.6	*OCA2, HERC2*	26

Angelman syndromes BP1-BP3	28537425				
15q24 BPA-BPC	chr15:72628218-75278711	2.521	74.73	*BBS4, STRA6, EDC3, MPI, COX5A*	40
15q11q13 BP3-BP5	chr15:28569118-32447357	2.521	59.79	*NSMCE3, FAN1, TRPM1*	21
7q11.23 distal	chr7:75456184-76629927	2.521	29.89	*POR, MDH2*	19

Regions are listed in descending order by population prevalence. Genes in the "Known recessive gene" column are ordered by coordinate map positions. Even though it is the third highest NAHR-mediated deletions, the Xp22.31-*STS* deletion is not included in this table because the current list focuses on autosomal recessive conditions. The gene *OTUD7A* in 15q13.3 BP4-BP5 is not reported as a recessive disease at the time of this study; however, patient analysis results from this study support this gene as a candidate recessive disease.

Table 2. Recessive genes with NAHR-mediated recurrent genomic deletions contributing to more than 20% of the overall disease burden.

Gene	Associated recessive disease	Region name	NAHR deletion frequency	NAHR-deletion Impact to Recessive Disease (NIRD)	Top 3 allele contribution to disease* (NAHR allele in red)	Fraction of NAHR allele frequency in all alleles	Aggregate carrier frequency
NPHP1	Nephronophthisis 1, juvenile, MIM# 256100	2q13 *NPHP1*	5.87E-03	7.7	***98***, 3, 2	85	6.89E-03
ADRA2B	Autosomal recessive mental retardation (from DECIPHER)	2q11.2	7.31E-05	4.1	***95***, 10, 10	90	8.12E-05
ALDOA	Glycogen storage disease XII, MIM# 611881	16p11.2 proximal	2.60E-04	4.1	***95***, 10, 10	90	2.88E-04
CEP19	Morbid obesity and spermatogenic failure, MIM# 615703	3q29	2.27E-05	4.1	***95***, 10, 10	90	2.52E-05
CORO1A	Immunodeficiency 8, MIM# 615401	16p11.2 proximal	2.60E-04	4.1	***95***, 10, 10	90	2.88E-04
COX5A	Mitochondrial complex IV deficiency, nuclear type 20, MIM# 619064	15q24 BPA-BPC	2.52E-06	4.1	***95***, 10, 10	90	2.80E-06
EDC3	Mental retardation, autosomal recessive 50, MIM# 616460	15q24 BPA-BPC	2.52E-06	4.1	***95***, 10, 10	90	2.80E-06
LAT	Immunodeficiency 52, MIM# 617514	16p11.2 distal	1.36E-04	4.1	***95***, 10, 10	90	1.51E-04
MIEF2	Combined oxidative phosphorylation	Smith Magenis	5.04E-06	4.1	***95***, 10, 10	90	5.60E-06

	deficiency 49, MIM# 619024	Syndrome					
SLC18A3	Myasthenic syndrome, congenital, 21, presynaptic, MIM# 617239	10q11.21q11.23	1.41E-04	4.1	***95***, 10, 10	90	1.57E-04
PMP22	Dejerine-Sottas disease, MIM# 145900	17p12 HNPP	3.15E-04	4.2	***94***, 11, 9	89	3.54E-04
OTUD7A	Neurodevelopmental disorder (this study)	15q13.3 BP4-BP5	9.33E-05	5.3	***93***, 10, 10	73	1.28E-04
RBM8A	Thrombocytopenia-absent radius syndrome, MIM# 274000	1q21.1 TAR	1.74E-04	9.8	***90***, 1, 1	90	1.93E-04
PRODH	Hyperprolinemia, type I, MIM# 239500	22q11.2 LCRA-D	1.77E-04	5	***87***, 36, 25	77	2.29E-04
UQCRC2	Mitochondrial complex III deficiency, nuclear type 5, MIM# 615160	16p12.1	5.92E-04	5.1	***86***, 49, 7	75	7.92E-04
NDE1	Lissencephaly 4 (with microcephaly), MIM# 614019	16p13.11	3.13E-04	5.1	***84***, 54, 15	72	4.31E-04
PEX11B	Peroxisome biogenesis disorder 14B, MIM# 614920	1q21 TAR	1.74E-04	4.7	***83***, 21, 18	71	2.44E-04
TUFM	Combined oxidative phosphorylation deficiency 4, MIM# 610678	16p11.2 distal	1.36E-04	3.9	***78***, 10, 10	64	2.11E-04
COX10	Mitochondrial complex IV deficiency, nuclear type 3, MIM# 619046	17p12 HNPP	3.15E-04	5.1	***77***, 48, 25	62	5.05E-04
SCARF2	Van den Ende-Gupta syndrome, MIM# 600920	22q11.2 LCRA-D	1.77E-04	4	***77***, 36, 7	62	2.84E-04
POLR3GL	Endosteal Hyperostosis and Oligodontia (from DECIPHER)	1q21 TAR	1.74E-04	4.1	***74***, 20, 13	59	2.95E-04
MYH11	Megacystis-microcolon-intestinal	16p13.11	3.13E-04	5	***72***, 24, 7	57	5.50E-04

	hypoperistalsis syndrome (from DECIPHER)						
NCAPH	Microcephaly 23, primary, autosomal recessive, MIM# 617985	2q11.2	7.31E-05	2.9	***71***, 27, 27	55	1.32E-04
PRRT2	Autosomal recessive mental retardation (from DECIPHER)	16p11.2 proximal	2.60E-04	5.3	***68***, 68, 10	52	5.02E-04
ANAPC1	Rothmund-Thomson syndrome, type 1, MIM# 618625	2q13	1.29E-04	3.9	***67***, 13, 11	50	2.57E-04
GRAP	Deafness, autosomal recessive 114, MIM# 618456	Smith Magenis Syndrome	5.04E-06	5.3	***67***, 85, 3	50	1.01E-05
CD19	Immunodeficiency, common variable, 3, MIM# 613493	16p11.2 distal	1.36E-04	4	***65***, 39, 28	48	2.84E-04
HJV	Hemochromatosis, type 2A, MIM# 602390	1q21 TAR	1.74E-04	5.2	***61***, 83, 5	44	3.92E-04
IGLL1	Agammaglobulinemia 2, MIM# 613500	22q11.2 LCRD-H	1.26E-05	5.2	***61***, 51, 50	44	2.87E-05
PIGW	Glycosylphosphatidylinositol biosynthesis defect 11, MIM# 616025	17q12	6.89E-05	5.2	***61***, 64, 35	44	1.56E-04
SLC25A1	Myasthenic syndrome, congenital, 23, presynaptic, MIM# 618197	22q11.2 LCRA-D	1.77E-04	4.5	***61***, 38, 15	43	4.08E-04
GP1BB	Giant platelet disorder, isolated, MIM# 231200	22q11.2 LCRA-D	1.77E-04	4.8	84, ***60***, 4	43	4.14E-04
RBP3	Retinitis pigmentosa 66, MIM# 615233	10q11.21q11.23	1.41E-04	4.1	***58***, 30, 9	41	3.44E-04
CNNM4	Jalili syndrome, MIM# 217080	2q11.2	7.31E-05	3.2	***57***, 16, 9	40	1.84E-04
FDFT1	Squalene synthase deficiency, MIM#	8p23.1	1.01E-05	5.1	***56***, 52, 52	39	2.58E-05

	618156						
SNAP29	Cerebral dysgenesis, neuropathy, ichthyosis, and palmoplantar keratoderma syndrome, MIM# 609528	22q11.2 LCRA-D	1.77E-04	4.5	***55***, 44, 28	38	4.62E-04
CDC45	Meier-Gorlin syndrome 7, MIM# 617063	22q11.2_LCRA-D	1.77E-04	4.5	***54***, 30, 19	37	4.73E-04
SGCG	Muscular dystrophy, limb-girdle, autosomal recessive 5, MIM# 253700	13q12.12	2.12E-04	4.7	***54***, 25, 15	37	5.73E-04
CHAT	Myasthenic syndrome, congenital, 6, presynaptic, MIM# 254210	10q11.21q11.23	1.41E-04	4.2	***52***, 25, 7	35	3.98E-04
NRROS	Seizures, early-onset, with neurodegeneration and brain calcification, MIM# 618875	3q29	2.27E-05	4.9	92, ***46***, 2	30	7.63E-05
NSMCE3	Lung disease, immunodeficiency, and chromosome breakage syndrome, MIM# 617241	15q11q13 BP3-BP4	3.53E-05	4.8	91, ***44***, 4	28	1.26E-04
TFRC	Immunodeficiency 46, MIM# 616740	3q29	2.27E-05	1.6	***40***, 41, 29	25	9.09E-05
PCYT1A	Spondylometaphyseal dysplasia with cone-rod dystrophy, MIM# 608940	3q29	2.27E-05	1.9	***38***, 39, 17	24	9.64E-05
SACS	Spastic ataxia, Charlevoix-Saguenay type, MIM# 270550	13q12.12	2.12E-04	4.4	***37***, 14, 13	23	9.20E-04
OTOA	Deafness, autosomal recessive 22, MIM# 607039	16p12.1	5.92E-04	4.4	80, ***35***, 5	21	2.78E-03
TXNRD2	Glucocorticoid deficiency 5, MIM#	22q11.2 LCRA-D	1.77E-04	3.7	48, ***35***, 36	21	8.25E-04

	617825						
MIPEP	Combined oxidative phosphorylation deficiency 31, MIM# 617228	13q12.12	2.12E-04	3.9	***33***, 15, 14	20	1.06E-03
PI4KA	Polymicrogyria, perisylvian, with cerebellar hypoplasia and arthrogryposis, MIM# 616531	22q11.2 LCRA-D	1.77E-04	4.7	***33***, 16, 13	20	9.07E-04
LMAN2L	Mental retardation, autosomal recessive, 52, MIM# 616887	2q11.2	7.31E-05	3.4	***32***, 32, 26	19	3.88E-04
TBX6	Spondylocostal dysostosis 5, MIM# 122600	16p11.2 proximal	2.60E-04	4.9	***32***, 27, 6	32	8.02E-04
ATP2A1	Brody myopathy, MIM# 601003	16p11.2 distal	1.36E-04	4.1	73, ***30***, 7	18	7.77E-04
DYNLT2B	Short-rib thoracic dysplasia 17 with or without polydactyly, MIM# 617405	3q29	2.27E-05	1.1	59, 43, ***28***	17	1.37E-04
TANGO2	Metabolic encephalomyopathic crises, recurrent, with rhabdomyolysis, cardiac arrhythmias, and neurodegeneration, MIM# 616878	22q11.2 LCRA-D	1.77E-04	2.9	78, ***27***, 23	15	1.14E-03
B9D1	Joubert syndrome 27, MIM# 617120	Smith Magenis Syndrome	5.04E-06	3.7	91, ***22***, 19	12	4.10E-05
ZNHIT3	PEHO syndrome, MIM# 260565	17q12	6.89E-05	3.7	96, ***22***, 2	13	5.47E-04
ERCC6	Cockayne syndrome, type B, MIM# 133540	10q11.21q11.23	1.41E-04	3.5	***21***, 15, 14	12	1.18E-03
FAN1	Interstitial nephritis, karyomegalic, MIM# 614817	15q13.3 BP4-BP5	9.33E-05	2.9	24, ***20***, 20	11	8.87E-04

LZTR1	Noonan syndrome 2, MIM# 605275	22q11.2 LCRA-D	1.77E-04	3.5	***20***, 17, 14	11	1.61E-03

*, the rows of the table are arranged in a descending order based on the NAHR deletion allele's contribution to the recessive disease, i.e. the percent of all affected individuals carrying at least one NAHR deletion allele, which are represented as the red numbers in the column "Top 3 allele contribution to disease". Note that the numbers from the column "Top 3 allele" are not disjunct events. For example, a patient can be compound heterozygous for the top 1 allele and the 2nd allele, and thus contribute to both numbers. Genes with an NAHR allele contribution to disease lower than 20% are not tabulated here, but can be found in Table S5.

Table 3. Clinically significant sequence variants uncovered by the deletions. Subjects #1 and #2 were identified in a *COX10*-phenotype-driven cohort analysis. Subjects #1, #3, and #4 were identified in the molecular-deletion-driven clinical exome data reanalysis.

ID	Deletion/ Allele frequency	Gene (RefSeq transcript)	Genic variant	Genomic coordinate (GRCh38)	MAF in gnomAD v3.1	Classification	Category
1	17p12 HNPP/ 3.148×10^{-4}	*COX10* (NM_001303.3)	c.1277_1282dup (p.M426_L427dup)	chr17:14207158_ 14207163dup	0	VUS	NDAC
2	17p12 HNPP/ 3.148×10^{-4}	*COX10* (NM_001303.3)	c.858G>T (p.W286C)	chr17:14192151G>T	6.567×10^{-6}	VUS	NDAC
3	10q11.21q11.23 deletion/ 1.412×10^{-4}	*ERCC6* (NM_000124.3)	c.1490T>C (p.F497S)	chr10:49505920A>G	0	VUS	NDAC
4	15q13.3 BP4-BP5 deletion/ 9.326×10^{-5}	*OTUD7A* (NM_130901.2)	c.2023_2066del (p.D675Hfs*188)	chr15:31484009_ 31484052del	6.58×10^{-5} [a]	VUS	NDGMC
5	16p11.2 proximal / 2.596×10^{-4}	*PRRT2* (NM_145239.2)	c.649dup (p.R217fs)	chr16: 29813703dup	1.472×10^{-4} [b]	Pathogenic	NDGMC

a. This variant is marked with “low complexity region” label in gnomAD, suggesting ambiguous variant call quality. It has a variant count of 2 in gnomAD v3.1. However, manual review of the alignment data from gnomAD suggest only 1 is of higher quality. The allele frequency is adjusted in half accordingly.

b. This variant is marked with “low complexity region” label in gnomAD, suggesting ambiguous variant call quality. It is located in a homopolymer region that is susceptible to false positive variant calling. The variant allele frequency quoted here may be overestimated.

Abbreviations: MAF, minor allele frequency; VUS, variant of unknow significance; NDAC, new disease allele characterization; NDGMC, new disease gene/mechanism characterization.

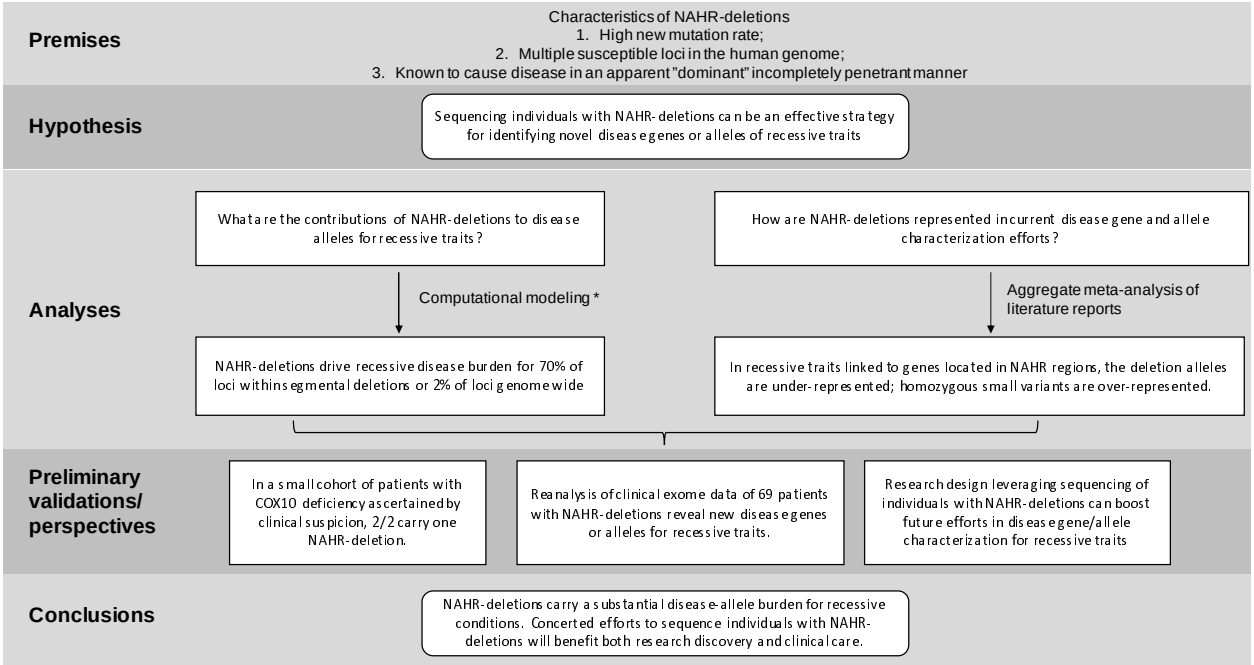

Figure 1. A flowchart of this study. Abbreviations: NAHR, non-allelic homologous recombination. *, a summary of the computational modeling is provided in Figure 2.

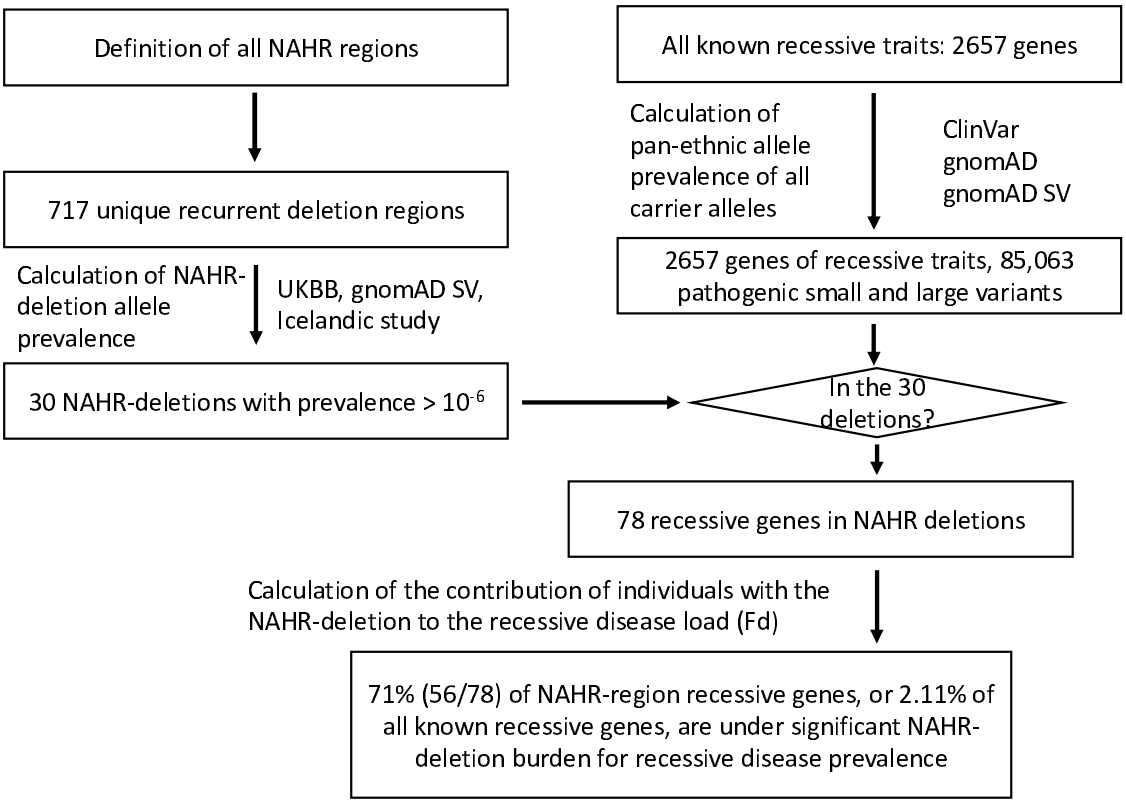

Figure 2. Computational modeling reveals unexpected contribution of NAHR-deletions to autosomal recessive disease trait burden.

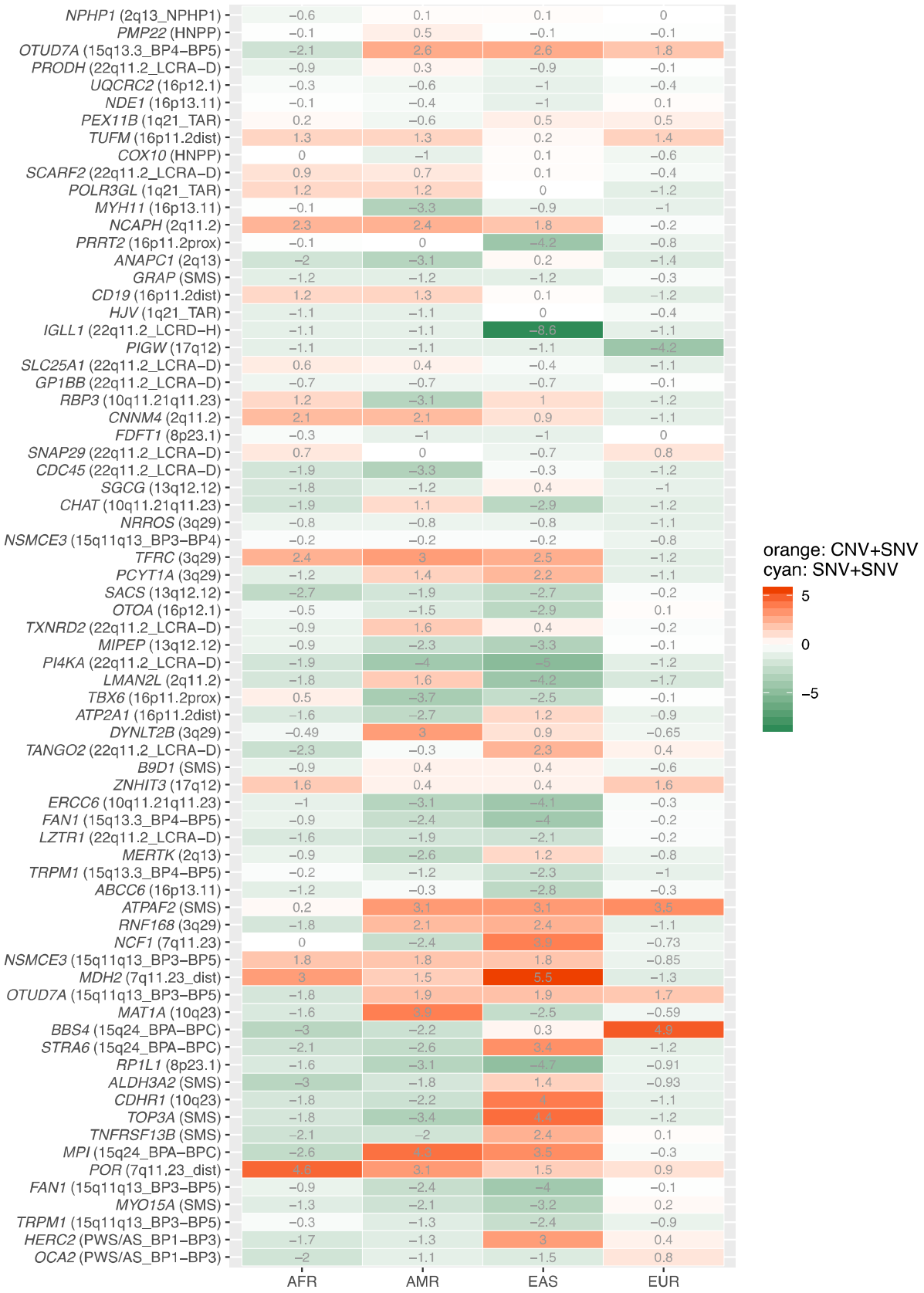
NPHP1 (2q13_NPHP1) −0.6 0.1 0.1 0
PMP22 (HNPP) −0.1 0.5 −0.1 −0.1
OTUD7A (15q13.3_BP4−BP5) −2.1 2.6 2.6 1.8
PRODH (22q11.2_LCRA−D) −0.9 0.3 −0.9 −0.1
UQCRC2 (16p12.1) −0.3 −0.6 −1 −0.4
NDE1 (16p13.11) −0.1 −0.4 −1 0.1
PEX11B (1q21_TAR) 0.2 −0.6 0.5 0.5
TUFM (16p11.2dist) 1.3 1.3 0.2 1.4
COX10 (HNPP) 0 −1 0.1 −0.6
SCARF2 (22q11.2_LCRA−D) 0.9 0.7 0.1 −0.4
POLR3GL (1q21_TAR) 1.2 1.2 0 −1.2
MYH11 (16p13.11) −0.1 −3.3 −0.9 −1
NCAPH (2q11.2) 2.3 2.4 1.8 −0.2
PRRT2 (16p11.2prox) −0.1 0 −4.2 −0.8
ANAPC1 (2q13) −2 −3.1 0.2 −1.4
GRAP (SMS) −1.2 −1.2 −1.2 −0.3
CD19 (16p11.2dist) 1.2 1.3 0.1 −1.2
HJV (1q21_TAR) −1.1 −1.1 0 −0.4
IGLL1 (22q11.2_LCRD−H) −1.1 −1.1 −8.6 −1.1
PIGW (17q12) −1.1 −1.1 −1.1 −4.2
SLC25A1 (22q11.2_LCRA−D) 0.6 0.4 −0.4 −1.1
GP1BB (22q11.2_LCRA−D) −0.7 −0.7 −0.7 −0.1
RBP3 (10q11.21q11.23) 1.2 −3.1 1 −1.2
CNNM4 (2q11.2) 2.1 2.1 0.9 −1.1
FDFT1 (8p23.1) −0.3 −1 −1 0
SNAP29 (22q11.2_LCRA−D) 0.7 0 −0.7 0.8
CDC45 (22q11.2_LCRA−D) −1.9 −3.3 −0.3 −1.2
SGCG (13q12.12) −1.8 −1.2 0.4 −1
CHAT (10q11.21q11.23) −1.9 1.1 −2.9 −1.2
NRROS (3q29) −0.8 −0.8 −0.8 −1.1
NSMCE3 (15q11q13_BP3−BP4) −0.2 −0.2 −0.2 −0.8
TFRC (3q29) 2.4 3 2.5 −1.2
PCYT1A (3q29) −1.2 1.4 2.2 −1.1
SACS (13q12.12) −2.7 −1.9 −2.7 −0.2
OTOA (16p12.1) −0.5 −1.5 −2.9 0.1
TXNRD2 (22q11.2_LCRA−D) −0.9 1.6 0.4 −0.2
MIPEP (13q12.12) −0.9 −2.3 −3.3 −0.1
PI4KA (22q11.2_LCRA−D) −1.9 −4 −5 −1.2
LMAN2L (2q11.2) −1.8 1.6 −4.2 −1.7
TBX6 (16p11.2prox) 0.5 −3.7 −2.5 −0.1
ATP2A1 (16p11.2dist) −1.6 −2.7 1.2 −0.9
DYNLT2B (3q29) −0.49 3 0.9 −0.65
TANGO2 (22q11.2_LCRA−D) −2.3 −0.3 2.3 0.4
B9D1 (SMS) −0.9 0.4 0.4 −0.6
ZNHIT3 (17q12) 1.6 0.4 0.4 1.6
ERCC6 (10q11.21q11.23) −1 −3.1 −4.1 −0.3
FAN1 (15q13.3_BP4−BP5) −0.9 −2.4 −4 −0.2
LZTR1 (22q11.2_LCRA−D) −1.6 −1.9 −2.1 −0.2
MERTK (2q13) −0.9 −2.6 1.2 −0.8
TRPM1 (15q13.3_BP4−BP5) −0.2 −1.2 −2.3 −1
ABCC6 (16p13.11) −1.2 −0.3 −2.8 −0.3
ATPAF2 (SMS) 0.2 3.1 3.1 3.5
RNF168 (3q29) −1.8 2.1 2.4 −1.1
NCF1 (7q11.23) 0 −2.4 3.9 −0.73
NSMCE3 (15q11q13_BP3−BP5) 1.8 1.8 1.8 −0.85
MDH2 (7q11.23_dist) 3 1.5 5.5 −1.3
OTUD7A (15q11q13_BP3−BP5) −1.8 1.9 1.9 1.7
MAT1A (10q23) −1.6 3.9 −2.5 −0.59
BBS4 (15q24_BPA−BPC) −3 −2.2 0.3 4.9
STRA6 (15q24_BPA−BPC) −2.1 −2.6 3.4 −1.2
RP1L1 (8p23.1) −1.6 −3.1 −4.7 −0.91
ALDH3A2 (SMS) −3 −1.8 1.4 −0.93
CDHR1 (10q23) −1.8 −2.2 4 −1.1
TOP3A (SMS) −1.8 −3.4 4.4 −1.2
TNFRSF13B (SMS) −2.1 −2 2.4 0.1
MPI (15q24_BPA−BPC) −2.6 4.3 3.5 −0.3
POR (7q11.23_dist) 4.6 3.1 1.5 0.9
FAN1 (15q11q13_BP3−BP5) −0.9 −2.4 −4 −0.1
MYO15A (SMS) −1.3 −2.1 −3.2 0.2
TRPM1 (15q11q13_BP3−BP5) −0.3 −1.3 −2.4 −0.9
HERC2 (PWS/AS_BP1−BP3) −1.7 −1.3 3 0.4
OCA2 (PWS/AS_BP1−BP3) −2 −1.1 −1.5 0.8
AFR
AMR
EAS
EUR
orange: CNV+SNV
cyan: SNV+SNV
5
0
−5

Figure 3. ΔNIRD scores for a population group relative to the general population. ΔNIRD is calculated by subtracting the general population NIRD from the specific population group NIRD. A positive ΔNIRD score suggests an even higher recessive disease contribution of the NAHR-deletion from that population group. A negative ΔNIRD score indicates a relatively higher probability for an affected patient to carry biallelic small variants in that population group. Genes that have zero ΔNIRD scores for all four population groups are not depicted in this heatmap.

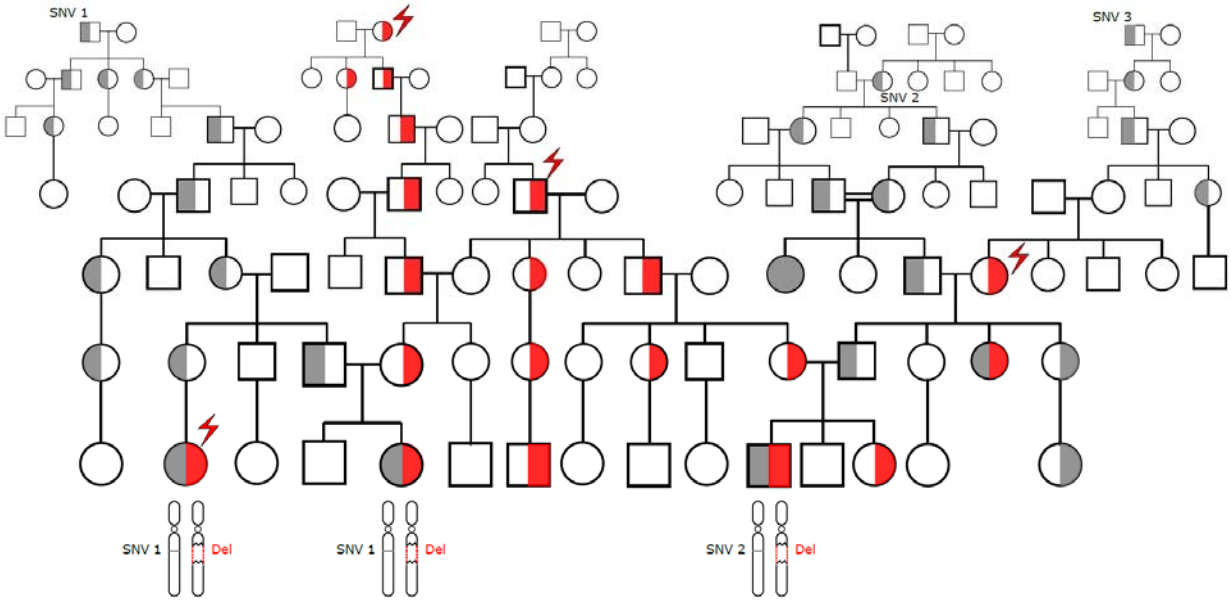

Figure 4. A 'segmental haploid genomics' approach for characterization of new disease genes or alleles for autosomal recessive conditions. The illustration above depicts dynamics of disease alleles in an autosomal recessive condition whose collective carrier burden is contributed by a recurrent genomic deletion (red area) and a few single nucleotide variants (SNVs, grey area). Individuals affected with biallelic pathogenic changes frequently carry the deletion as one of the two alleles, because the deletion arises recurrently in multiple lineages (indicated by the red lightning bolt arrow). SNV disease alleles for recessive genes tend to be passed on from ancestral generations, and may drift away without being noticed if they do not converge with another disease allele (SNV3). However, they may emerge to medical attention frequently in families with high degree of autozygosity, as illustrated in generations 3 and 4 for SNV2.

Supplemental Figure and Table legends

Figure S1. Genome-wide map for all predicted NAHR recurrent genomic deletions. Each predicted deletion event is marked as a green horizontal bar below the chromosome ideograms. The vertical bars above the chromosome ideograms illustrates the density for segmental duplications in a 1000-bp moving window.

Figure S2. Compound heterozygous HNPP deletion and *COX10* variant leading to recessive COX10 deficiency in Subjects #2 and #3. **A.** The *COX10* gene spans the repeat sequence that mediate the recurrent HNPP deletion at chromosome 17p12. The *COX10* variant in the Subject #2 is located at the 3' end of the *COX10* gene on exon 7, which is inside the HNPP deletion interval. The *COX10* variant in the Subject #3 is located at the *COX10* gene exon 7, which is embedded in a CMT1A-REP. Red segments, exons of the *COX10* gene; yellow arrows, CMT1A-REPs; thunderbolts, *COX10* variants observed in Subject #2 and #3, respectively. **B.** Diagram illustrating the scheme of the relationship between the SNV/indel and recurrent deletion identified in Subject #2 and #3.

Table S1. All 717 recurrent genomic deletions predicted based on the repeat structure in the human reference genome GRCh38.

Table S2. All clinically reported recurrent deletions and their prevalance estimates.

Table S3. Carrier disease allele frequencies by allele.

Table S4. Carrier allele frequency burden by gene. The list is ranked by genes from the highest burden to the lowest burden. The frequency burden in this list only includes the actual observed variants; the 10% extra hypothetical uncharacterized alleles as described in the Methods section are not included.

Table S5. Gene-level NAHR contribution to carrier allele and recessive disease burden as well as NAHR Deletion Impact to Recessive Traits (DIRT). This table is comprised of five panels, representing results generated using data from the general population and four specific ethnic groups, including African (AFR), Latino (AMR), East Asian (EAS), and European (EUR).

Table S6. Meta-analyses for literature reported patients affected with the 13 recessive disorders contributed by significant NAHR-mediated deletion burden.

Table S7. Molecular findings of recurrent deletions identified from clinical exome sequencing.

Table S8. Literature review for 15q13.3 recurrent deletions.

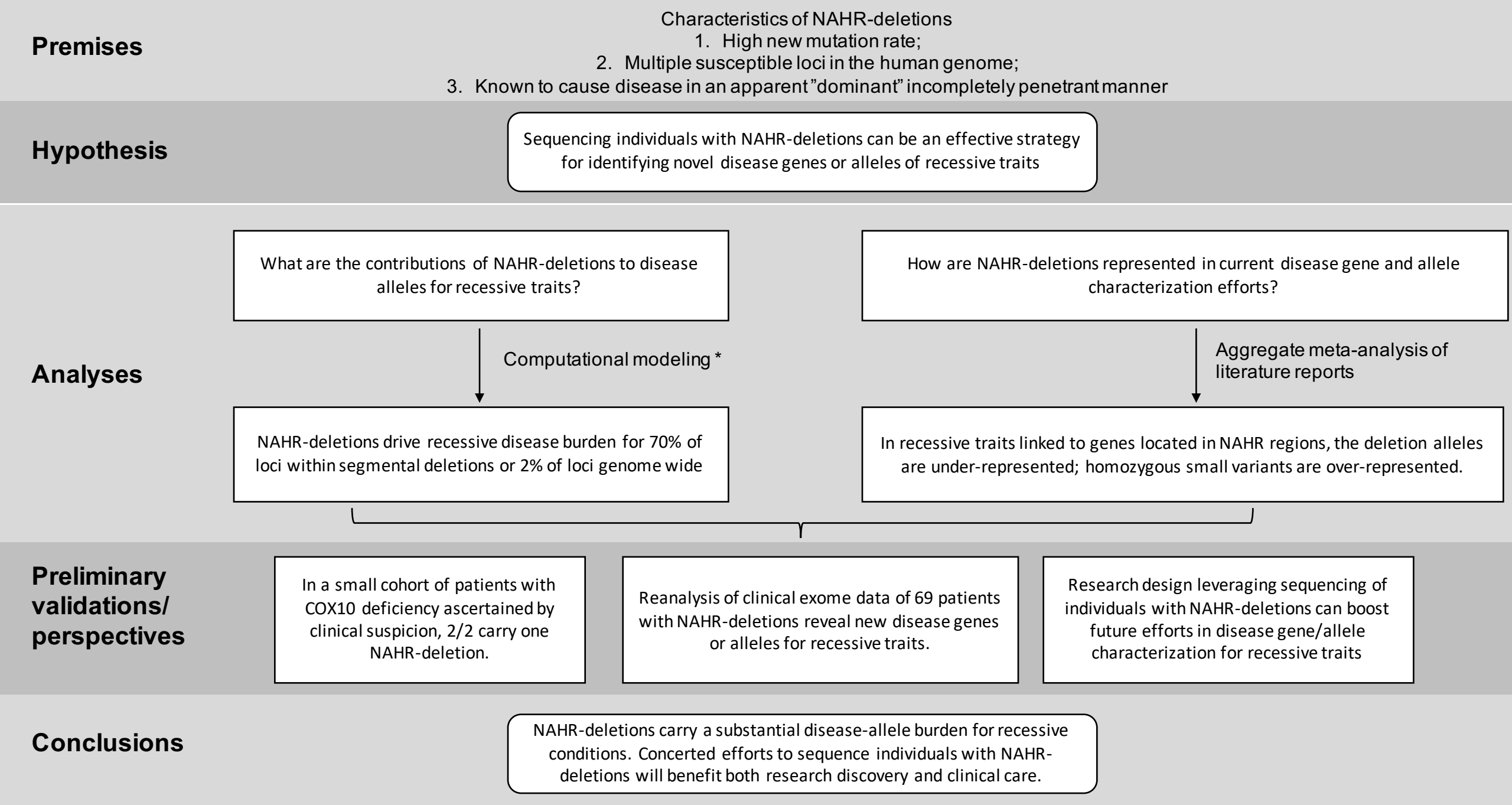
Premises
Characteristics of NAHR-deletions
1. High new mutation rate;
2. Multiple susceptible loci in the human genome;
3. Known to cause disease in an apparent "dominant" incompletely penetrant manner
Hypothesis
Sequencing individuals with NAHR-deletions can be an effective strategy for identifying novel disease genes or alleles of recessive traits
Analyses
What are the contributions of NAHR-deletions to disease alleles for recessive traits?
Computational modeling *
NAHR-deletions drive recessive disease burden for 70% of loci within segmental deletions or 2% of loci genome wide
How are NAHR-deletions represented in current disease gene and allele characterization efforts?
Aggregate meta-analysis of literature reports
In recessive traits linked to genes located in NAHR regions, the deletion alleles are under-represented; homozygous small variants are over-represented.
Preliminary validations/ perspectives
In a small cohort of patients with COX10 deficiency ascertained by clinical suspicion, 2/2 carry one NAHR-deletion.
Reanalysis of clinical exome data of 69 patients with NAHR-deletions reveal new disease genes or alleles for recessive traits.
Research design leveraging sequencing of individuals with NAHR-deletions can boost future efforts in disease gene/allele characterization for recessive traits
Conclusions
NAHR-deletions carry a substantial disease-allele burden for recessive conditions. Concerted efforts to sequence individuals with NAHR-deletions will benefit both research discovery and clinical care.

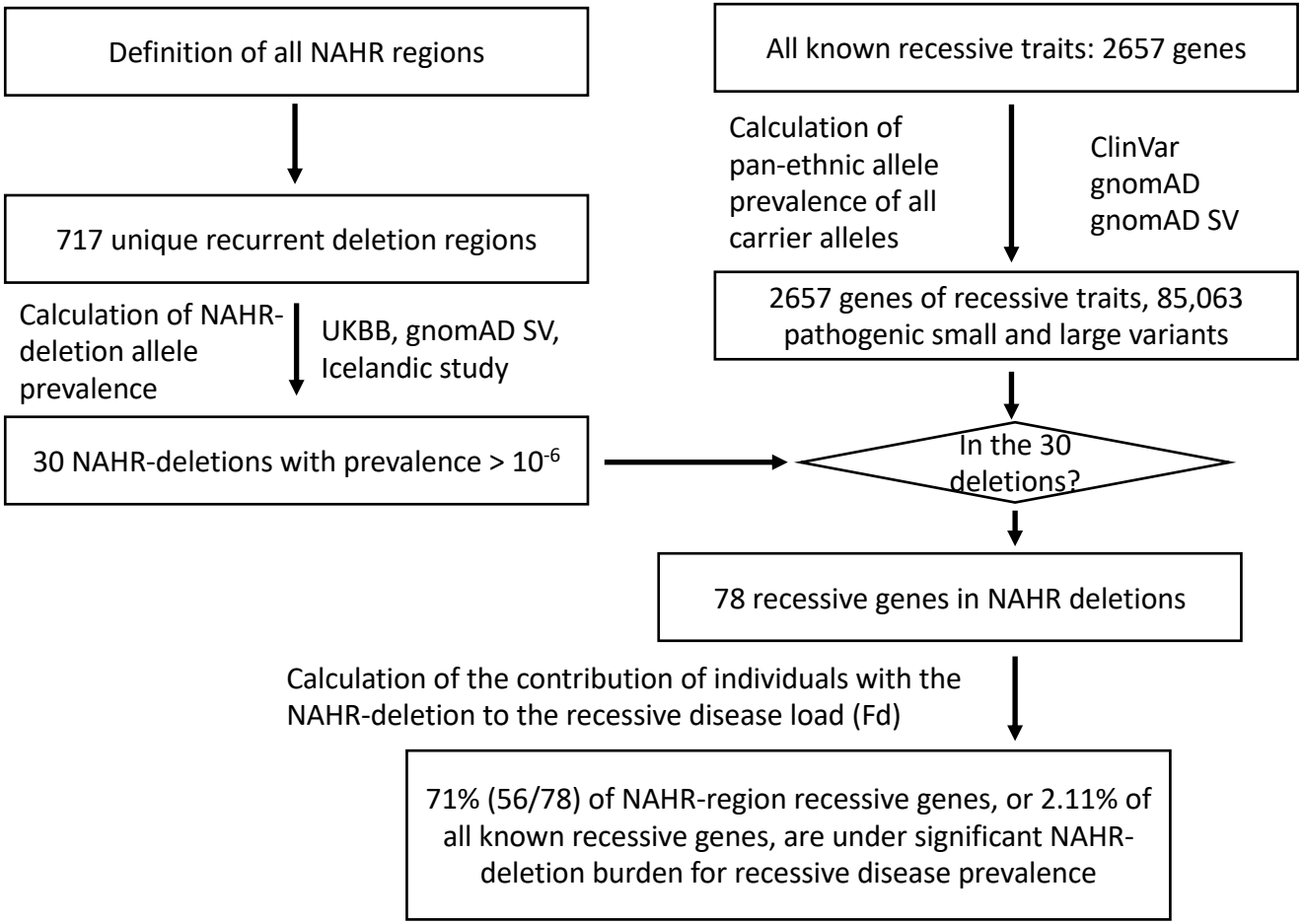
Definition of all NAHR regions
717 unique recurrent deletion regions
Calculation of NAHR-deletion allele prevalence
UKBB, gnomAD SV, Icelandic study
30 NAHR-deletions with prevalence > 10^{-6}
All known recessive traits: 2657 genes
Calculation of pan-ethnic allele prevalence of all carrier alleles
ClinVar
gnomAD
gnomAD SV
2657 genes of recessive traits, 85,063 pathogenic small and large variants
In the 30 deletions?
78 recessive genes in NAHR deletions
Calculation of the contribution of individuals with the NAHR-deletion to the recessive disease load (Fd)
71% (56/78) of NAHR-region recessive genes, or 2.11% of all known recessive genes, are under significant NAHR-deletion burden for recessive disease prevalence

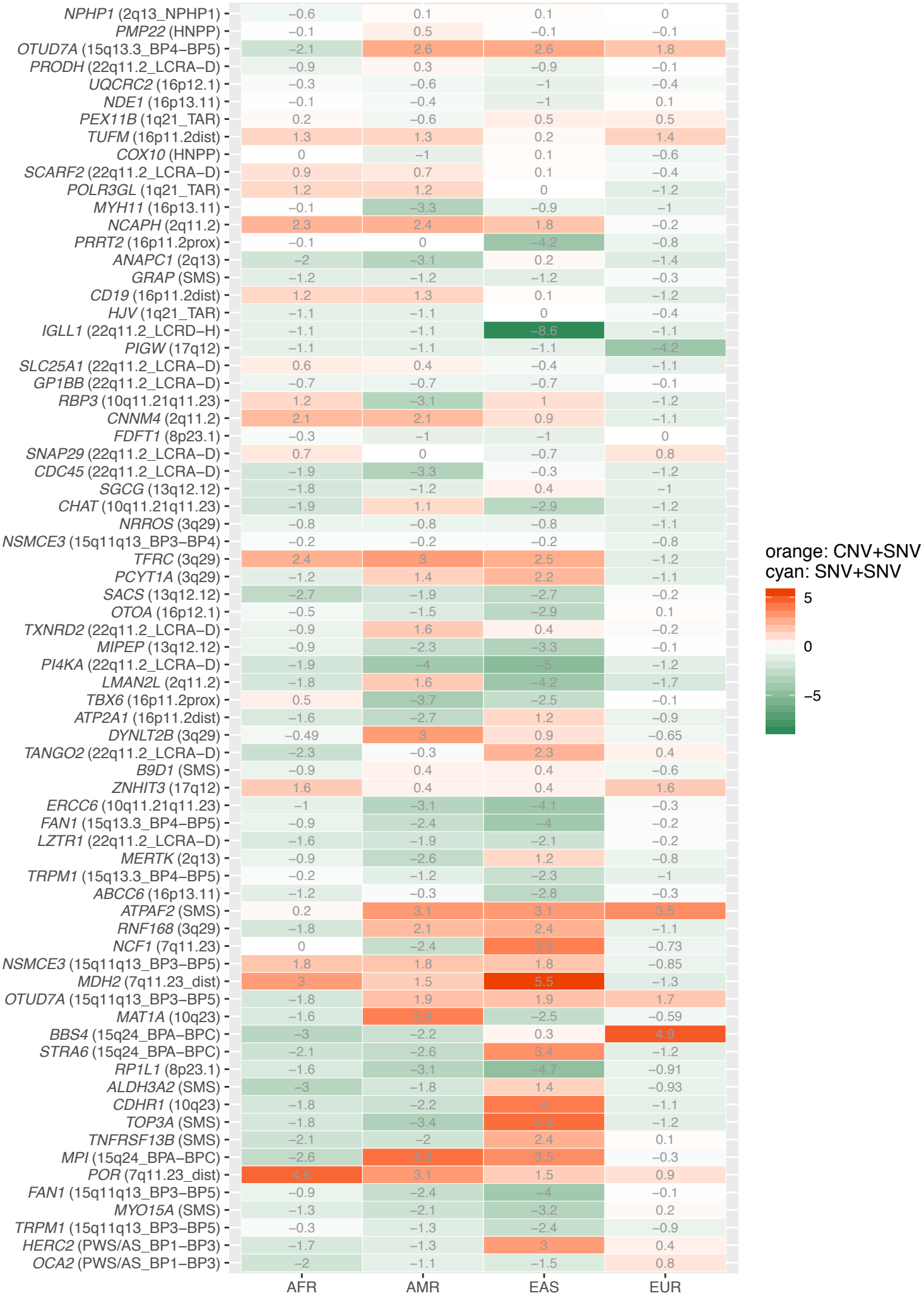
NPHP1 (2q13_NPHP1) −0.6 0.1 0.1 0
PMP22 (HNPP) −0.1 0.5 −0.1 −0.1
OTUD7A (15q13.3_BP4−BP5) −2.1 2.6 2.6 1.8
PRODH (22q11.2_LCRA−D) −0.9 0.3 −0.9 −0.1
UQCRC2 (16p12.1) −0.3 −0.6 −1 −0.4
NDE1 (16p13.11) −0.1 −0.4 −1 0.1
PEX11B (1q21_TAR) 0.2 −0.6 0.5 0.5
TUFM (16p11.2dist) 1.3 1.3 0.2 1.4
COX10 (HNPP) 0 −1 0.1 −0.6
SCARF2 (22q11.2_LCRA−D) 0.9 0.7 0.1 −0.4
POLR3GL (1q21_TAR) 1.2 1.2 0 −1.2
MYH11 (16p13.11) −0.1 −3.3 −0.9 −1
NCAPH (2q11.2) 2.3 2.4 1.8 −0.2
PRRT2 (16p11.2prox) −0.1 0 −4.2 −0.8
ANAPC1 (2q13) −2 −3.1 0.2 −1.4
GRAP (SMS) −1.2 −1.2 −1.2 −0.3
CD19 (16p11.2dist) 1.2 1.3 0.1 −1.2
HJV (1q21_TAR) −1.1 −1.1 0 −0.4
IGLL1 (22q11.2_LCRD−H) −1.1 −1.1 −8.6 −1.1
PIGW (17q12) −1.1 −1.1 −1.1 −4.2
SLC25A1 (22q11.2_LCRA−D) 0.6 0.4 −0.4 −1.1
GP1BB (22q11.2_LCRA−D) −0.7 −0.7 −0.7 −0.1
RBP3 (10q11.21q11.23) 1.2 −3.1 1 −1.2
CNNM4 (2q11.2) 2.1 2.1 0.9 −1.1
FDFT1 (8p23.1) −0.3 −1 −1 0
SNAP29 (22q11.2_LCRA−D) 0.7 0 −0.7 0.8
CDC45 (22q11.2_LCRA−D) −1.9 −3.3 −0.3 −1.2
SGCG (13q12.12) −1.8 −1.2 0.4 −1
CHAT (10q11.21q11.23) −1.9 1.1 −2.9 −1.2
NRROS (3q29) −0.8 −0.8 −0.8 −1.1
NSMCE3 (15q11q13_BP3−BP4) −0.2 −0.2 −0.2 −0.8
TFRC (3q29) 2.4 3 2.5 −1.2
PCYT1A (3q29) −1.2 1.4 2.2 −1.1
SACS (13q12.12) −2.7 −1.9 −2.7 −0.2
OTOA (16p12.1) −0.5 −1.5 −2.9 0.1
TXNRD2 (22q11.2_LCRA−D) −0.9 1.6 0.4 −0.2
MIPEP (13q12.12) −0.9 −2.3 −3.3 −0.1
PI4KA (22q11.2_LCRA−D) −1.9 −4 −5 −1.2
LMAN2L (2q11.2) −1.8 1.6 −4.2 −1.7
TBX6 (16p11.2prox) 0.5 −3.7 −2.5 −0.1
ATP2A1 (16p11.2dist) −1.6 −2.7 1.2 −0.9
DYNLT2B (3q29) −0.49 3 0.9 −0.65
TANGO2 (22q11.2_LCRA−D) −2.3 −0.3 2.3 0.4
B9D1 (SMS) −0.9 0.4 0.4 −0.6
ZNHIT3 (17q12) 1.6 0.4 0.4 1.6
ERCC6 (10q11.21q11.23) −1 −3.1 −4.1 −0.3
FAN1 (15q13.3_BP4−BP5) −0.9 −2.4 −4 −0.2
LZTR1 (22q11.2_LCRA−D) −1.6 −1.9 −2.1 −0.2
MERTK (2q13) −0.9 −2.6 1.2 −0.8
TRPM1 (15q13.3_BP4−BP5) −0.2 −1.2 −2.3 −1
ABCC6 (16p13.11) −1.2 −0.3 −2.8 −0.3
ATPAF2 (SMS) 0.2 3.1 3.1 3.5
RNF168 (3q29) −1.8 2.1 2.4 −1.1
NCF1 (7q11.23) 0 −2.4 3.9 −0.73
NSMCE3 (15q11q13_BP3−BP5) 1.8 1.8 1.8 −0.85
MDH2 (7q11.23_dist) 3 1.5 5.5 −1.3
OTUD7A (15q11q13_BP3−BP5) −1.8 1.9 1.9 1.7
MAT1A (10q23) −1.6 3.9 −2.5 −0.59
BBS4 (15q24_BPA−BPC) −3 −2.2 0.3 4.9
STRA6 (15q24_BPA−BPC) −2.1 −2.6 3.4 −1.2
RP1L1 (8p23.1) −1.6 −3.1 −4.7 −0.91
ALDH3A2 (SMS) −3 −1.8 1.4 −0.93
CDHR1 (10q23) −1.8 −2.2 4 −1.1
TOP3A (SMS) −1.8 −3.4 4.4 −1.2
TNFRSF13B (SMS) −2.1 −2 2.4 0.1
MPI (15q24_BPA−BPC) −2.6 4.3 3.5 −0.3
POR (7q11.23_dist) 4.6 3.1 1.5 0.9
FAN1 (15q11q13_BP3−BP5) −0.9 −2.4 −4 −0.1
MYO15A (SMS) −1.3 −2.1 −3.2 0.2
TRPM1 (15q11q13_BP3−BP5) −0.3 −1.3 −2.4 −0.9
HERC2 (PWS/AS_BP1−BP3) −1.7 −1.3 3 0.4
OCA2 (PWS/AS_BP1−BP3) −2 −1.1 −1.5 0.8
AFR
AMR
EAS
EUR
orange: CNV+SNV
cyan: SNV+SNV
5
0
−5

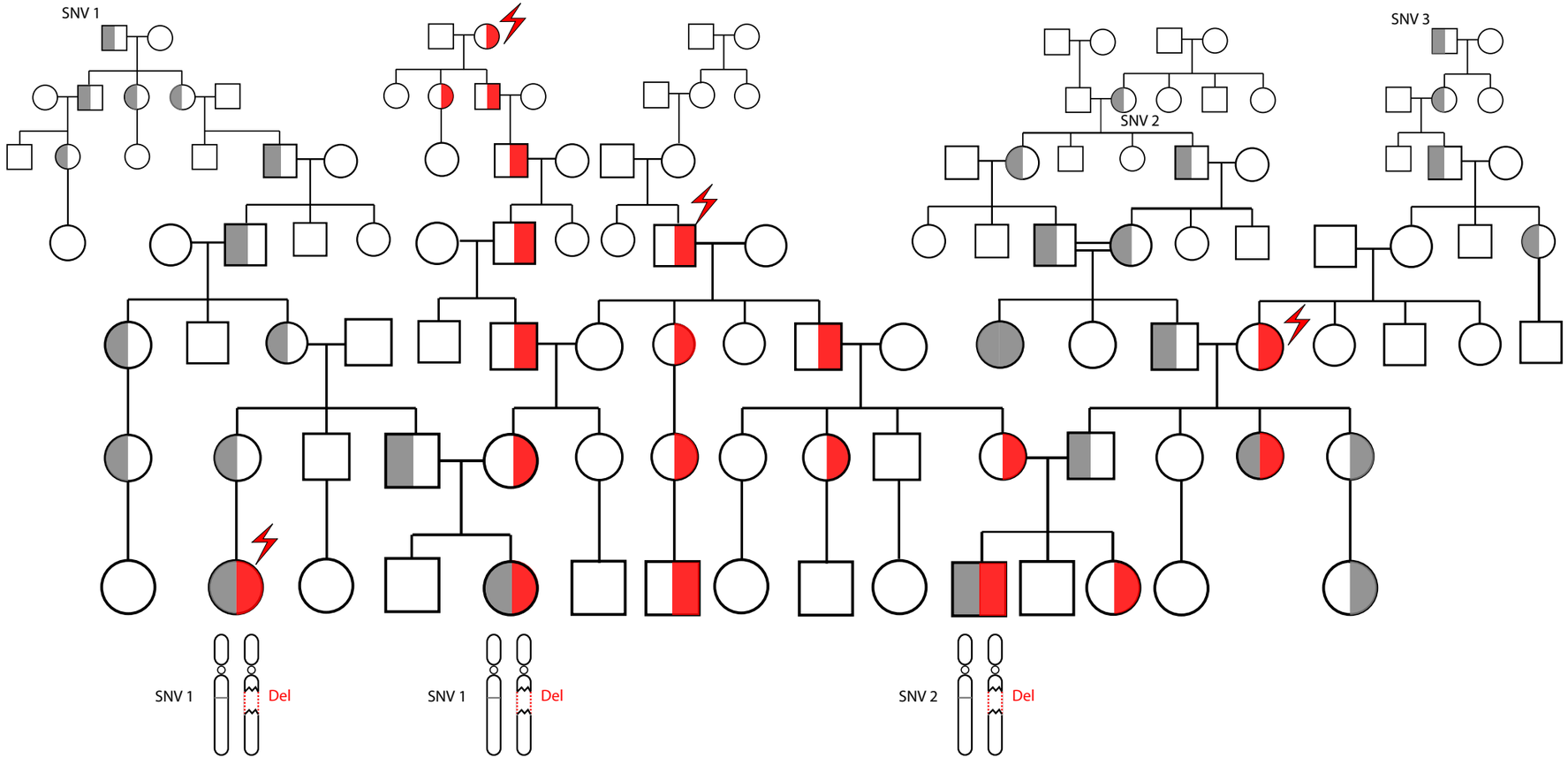
SNV 1
SNV 2
SNV 3
SNV 1
Del
SNV 1
Del
SNV 2
Del